

Introduction to Time-Frequency Signal Analysis

Boualem Boashash
Braham Barkat

ABSTRACT Time-frequency signal analysis (TFSA) has developed as a significant field in the area of signal processing. It involves the representation and processing of signals with time-varying spectral characteristics. This chapter presents fundamental principles of TFSA and reviews the main contributions to the field, including the most recent advances, such as polynomial Wigner–Ville distributions (PWVD), the high time-frequency resolution B-distribution, and the instantaneous frequency tracking and estimation.

11.1 Introduction

The field of time-frequency signal analysis (TFSA) is one of the recent developments which provides suitable tools for analyzing nonstationary signals occurring in many fields of engineering, such as telecommunications, radar, sonar, vibration analysis, biomedicine, speech, and seismic exploration. Nonstationary signals are characterized by a time-varying spectral content. This chapter shows how to deal with such signals using a TFSA approach; it outlines many of the important concepts underpinning TFSA, and includes an historical perspective of their development. The chapter builds upon and refines concepts and results that were originally reported in [1] to [7]. Since then, some important recent developments have occurred which point toward the need to present a unified approach to areas which are too often seen by some as unrelated. Examples are notions of instantaneous frequency and group delay, ambiguity functions, “higher-order spectra,” and others. This chapter attempts to introduce the field of TFSA within this “unified” perspective and presents some new important developments that are relevant to practitioners in the field.

Important original developments in TFSA can be traced back to the end of the 1940s [8], [9]. Since then, very few researchers became interested in the field [10]–[13] until a surge of interest occurred in the 1980s. The beginning of that decade saw pioneering efforts in various parts of the world at developing TFSA-based spectral analysis techniques for nonstationary signals, in order to overcome the drawbacks of classical spectral analysis [14]–[19].

These drawbacks arise because the classical spectral analysis tool, the Fourier transform (FT), implicitly assumes that the spectral characteristics of the signal are time-invariant, when in reality, real-life signals, both natural and man-made, almost always exhibit some degree of nonstationarity. When the important spectral features of the signals are time-varying, Fourier analysis produces an averaged (i.e., smeared or distorted) spectral representation, which leads to a loss in frequency resolution. One way to deal with the spectral smearing is to reduce the effects of the variation in time by taking the spectral estimates over adjacent short-time intervals of the signal, centered about particular time instants (a short-time Fourier transform) (STFT). Unfortunately, the shortened observation window produces a problem of its own: smearing caused by the “uncertainty relationship” of time and band-limited signals [8].

An equivalent way to deal with the problem of nonstationarity is to pass the signals through a filter bank composed of adjacent narrow-band bandpass filters, followed by a further spectral analysis of the output of each filter (a method referred to as “sonograph”). Again, the same problem described above occurs: the uncertainty principle [8] is encountered this time as a result of the band limitations of the filters. If small bandwidth filters are used, the ability to localize signal features well in time is lost. If large bandwidth filters are used, the fine-time domain detail can be obtained, but the frequency resolution becomes poor.

A major theoretical breakthrough in the field of time-frequency was accomplished by the scientist Wigner in the context of quantum mechanics. Wigner’s work was later introduced in the signal analysis context by Ville. This joint time-frequency distribution was referred to as Wigner–Ville distribution (WVD). The WVD has a high spectral resolution and is optimal, in the sense of energy concentration around the signal instantaneous frequency (IF), for linear frequency modulated (FM) signals (for FM signals, the IF describes the FM law). However, the WVD had not been applied to real-life problems until it was implemented by Boashash in the late 1970s in the context of linear FM signal analysis for seismic prospecting [20]. This practical breakthrough resulted in a renewed interest for time-frequency analysis in engineering.

Even though the WVD has a high time-frequency resolution, it has also a fundamental drawback: cross-term interferences and/or artifacts. In addition to the auto-terms, the WVD presents some cross-terms for multicomponent signals (composite signals that consist of a sum of monocomponent signals [1]) and artifacts for monocomponent nonlinear FM signals. These artifacts can hide the real features of the analyzed signal which often make the use of the WVD difficult for a nonspecialist. In order to overcome the WVD limitation for multicomponent signals, researchers proposed new time-frequency distributions (TFDs). Some of the most popular ones are the reduced interference distributions (RIDs) which were shown to be an extension of the WVD [21]. These distributions along with the WVD and the spectrogram form a class of quadratic TFDs. On the other hand, a windowed version of the WVD was proposed to reduce artifacts in the analysis of monocomponent nonlinear FM signals but the resulting distribution is known to have lower spectral resolution [22]. In order to keep maximum resolution for

nonlinear FM signals, Boashash and coworkers proposed the polynomial Wigner–Ville distribution (PWVD) [23]. This distribution is optimal, in the sense of energy concentration around the IF, for polynomial FM signals, and can be viewed as an extension of the WVD.

In many real-life applications, the IF characterizes important physical parameters of the signals; therefore, it is desirable to have effective methods for IF estimation. The IF estimation of nonstationary signals is as important as their representation in the joint time-frequency domain. A well-known class of nonparametric methods, for IF estimation, is based on using the peak of TFDs. Some recent results in IF estimation using the PWVD are given in the last section of this chapter.

The chapter is organized as follows. In Section 11.2, we discuss signal representations and the need for time-frequency analysis as opposed to either time or frequency analysis. In Section 11.3, we present some early theoretical foundations of TFSA. In Section 11.4, we present the class of quadratic TFDs and discuss its relationship to two-dimensional filtering in the ambiguity domain. In Section 11.5, we present tools for TFSA of nonlinear FM signals using the PWVD and related methods such as time-varying higher-order spectra.

11.2 Fundamental Signal Representations

11.2.1 Signal models

Defining a signal model is often an important step in the process of solving practical engineering problems. An example of a step-by-step procedure is:

1. Understand the physical problem and derive a physical model.
2. Determine the corresponding signal model.
3. Work out the relationship between the parameters of the signal model and the parameters of the physical model.
4. Construct the algorithm needed to estimate the signal model parameters from the observations.

Six possible signal models are defined below, ranging from the most simplistic case of a single sinusoid to more general situations:

- Single sinusoid:

$$s_1(t) = \cos(2\pi f_c t). \quad (11.2.1)$$

- Multicomponent, stationary sinusoid:

$$s_2(t) = \sum_{k=1}^M a_k \cos(2\pi f_k t). \quad (11.2.2)$$

- Single component, nonstationary signal:

$$s_3(t) = e^{j2\pi \int_0^t f(\tau)d\tau}. \quad (11.2.3)$$

- Multicomponent, nonstationary signal:

$$s_4(t) = \sum_{k=1}^M a_k e^{j2\pi \int_0^t f_k(\tau)d\tau}. \quad (11.2.4)$$

- Multicomponent, nonstationary signal in additive noise, $w(t)$:

$$s_5(t) = \sum_{k=1}^M a_k e^{j2\pi \int_0^t f_k(\tau)d\tau} + w(t). \quad (11.2.5)$$

- Multicomponent, nonstationary signal in additive noise, $w(t)$, and multiplicative noise, $m_k(t)$:

$$s_6(t) = \sum_{k=1}^M m_k(t) e^{j2\pi \int_0^t f_k(\tau)d\tau} + w(t). \quad (11.2.6)$$

Note that for $s_1(t)$ we only require one parameter, frequency, to completely characterize the signal. For $s_2(t)$ we require $2M$ parameters: the relative amplitudes and frequencies of each component.

As discussed above, the signal model is very important in algorithm development. From the model we can select the signal parameter which we wish to estimate. It is then necessary to choose an appropriate tool. The choice of the tool depends greatly on the signal model. For example, if our signal models are either $s_1(t)$ or $s_2(t)$ then the FT is the most appropriate tool. There is no point in using a more complex tool, such as the spectrogram, since the FT will perform the required task adequately. However, for $s_3(t)$ the FT would not be adequate so we would need to consider an alternative such as the spectrogram or the WVD. For a signal model such as $s_5(t)$, even more advanced techniques will be needed. Some of these techniques will be covered in this chapter.

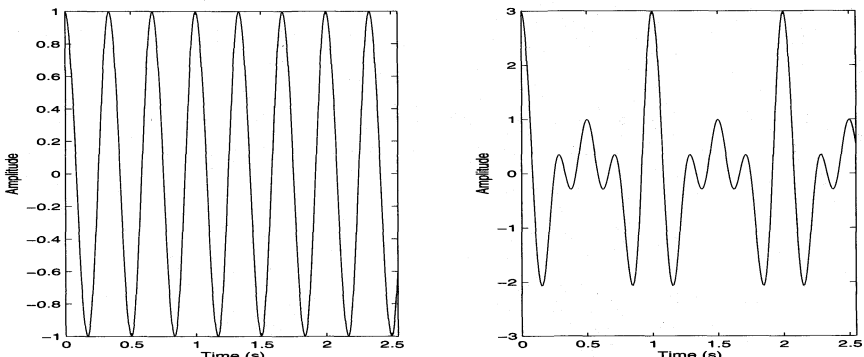
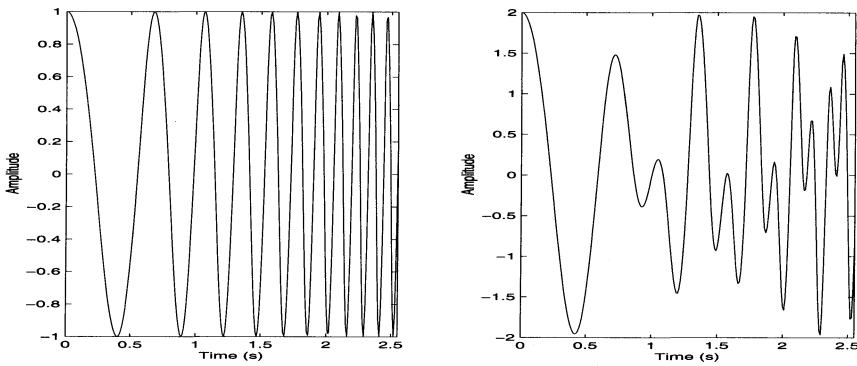
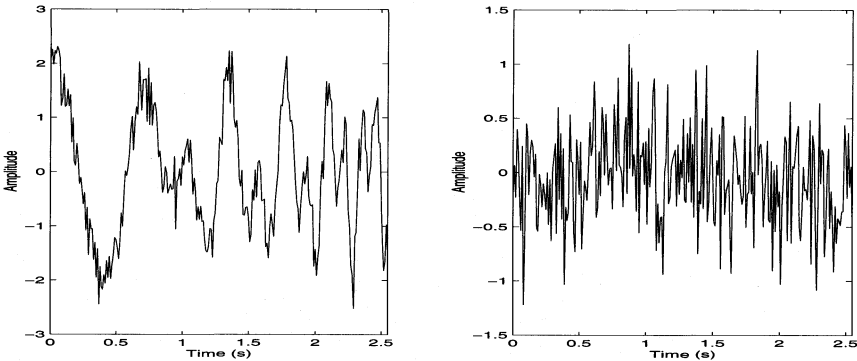


FIGURE 11.1. Signals corresponding to $s_1(t)$ and $s_2(t)$.

FIGURE 11.2. Signals corresponding to $s_3(t)$ and $s_4(t)$.FIGURE 11.3. Signals corresponding to $s_5(t)$ and $s_6(t)$.

11.2.2 Need for a joint time-frequency analysis

There are two classical representations for signal analysis. One is based on the temporal representation of the signal, $s(t)$, and the other is based on its spectral representation, defined by the FT, $S(f)$ as

$$S(f) = \int_{-\infty}^{+\infty} s(t)e^{-j2\pi ft} dt. \quad (11.2.7)$$

The time domain representation reveals information about the actual presence of the signal, its strengths and temporal evolution. The FT indicates which frequencies are present in the signal and their relative magnitudes. To characterize deterministic signals, in practice, one may use the instantaneous energy (i.e., the squared modulus of the time signal) or the energy spectrum (the squared modulus of the FT of the signal). For random signals, one may use the autocorrelation (time domain) or its FT, the power spectrum. These analysis tools provide solutions for many problems related to stationary signals. However, they have immediate limitations when applied to nonstationary signals; i.e., to signals whose spectral content varies

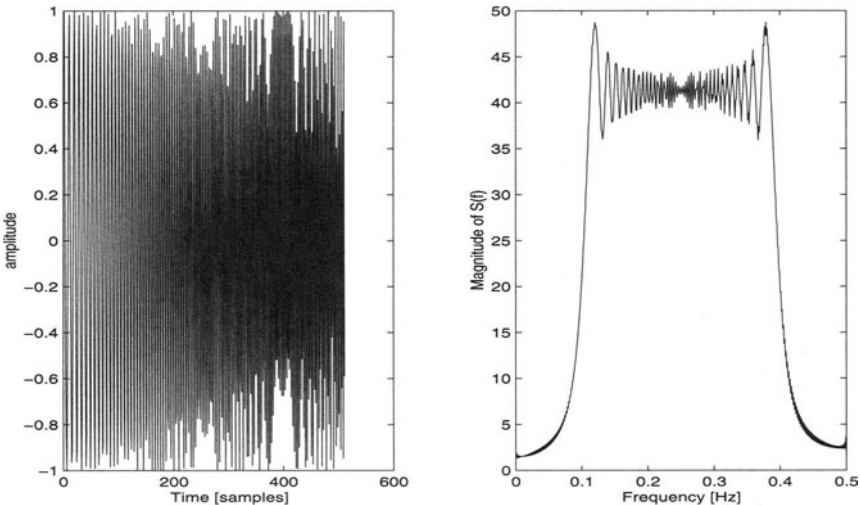


FIGURE 11.4. Time domain representation (left) of the linear FM signal $s(t)$ and its spectrum (right).

with time. For instance, the spectrum gives no indication as to how the frequency content of the signal changes with time, information which is needed when one deals with signals such as FM signals. The chirp signal is an example of such a signal. It is a linear FM signal, used, for example, as a controllable source in seismic processing and radar. It is analogous to a musical note with a steadily rising pitch, and is of the form

$$s(t) = \text{rect}\left(\frac{t - T/2}{T}\right) \cos\left[2\pi\left(f_0 t + \alpha \frac{t^2}{2}\right)\right], \quad (11.2.8)$$

where $\text{rect}(t/T)$ is 1 for $|t| \leq T/2$ and zero elsewhere, f_0 is the center frequency, and α represents the rate of the frequency change.

The fact that the frequency in the signal is steadily rising with time is not revealed by the signal spectrum displayed in Figure 11.4; it only reveals a broadband spectrum.

A more elegant way to reveal the time and frequency dependence of the signal, $s(t)$, is to use a joint TFD as in Figure 11.5. The start and stop times are easily identifiable, as is the variation of the spectral behavior of the signal. This information cannot be retrieved from either the instantaneous energy or the spectrum representations. It is lost when the FT is squared and the phase of the spectrum is thereby discarded. The phase spectrum actually contains this information about “the internal organization” of the signal, as physically displayed in Figure 11.5. This “internal organization” includes such details as times at which the signal has energy above or below a particular threshold, and the order of appearance in time of the different frequencies present. The difficulty of interpreting and analyzing a phase spectrum makes the concept of a joint time-frequency signal representation

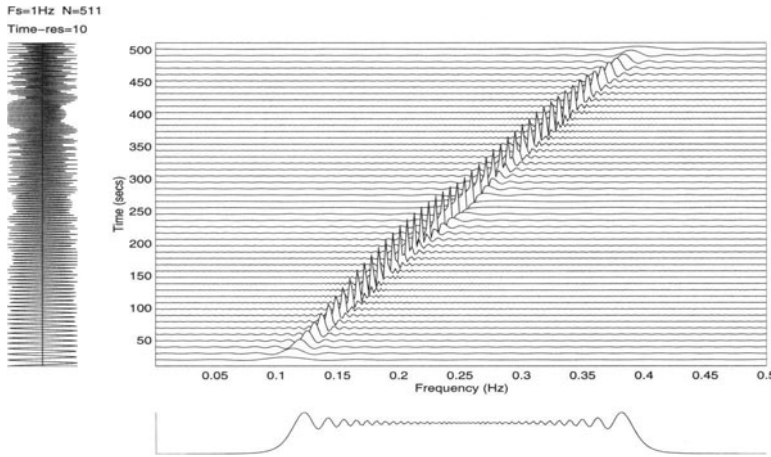


FIGURE 11.5. Time-frequency representation of the linear FM signal $s(t)$: the signal's time domain representation appears on the left, and its spectrum on the bottom.

attractive. For example, a musician would prefer to interpret a piece of music, which shows the pitch, start time, and duration of the notes to be played rather than to be given a magnitude and phase spectrum of that piece of music to decipher [24].

Another example of the limitation of the FT analysis is illustrated by the following. Consider two random signals, $x_1(t)$ and $x_2(t)$, which are realizations of the process $X_i(t) = S_i(t) + N(t)$, $i = 1, 2$, where $S_i(t)$ is deterministic and $N(t)$ is a zero-mean white Gaussian noise process. The deterministic signals, $S_1(t)$ and $S_2(t)$, are defined as

$$S_1(t) = \text{rect}\left(\frac{t}{T}\right) \cos\left[2\pi\left(f_0 t + \frac{\alpha}{2} t^2\right)\right] \quad (\text{linear FM}), \quad (11.2.9)$$

$$S_2(t) = \frac{\sin(\pi B t)}{\pi t} \cos(2\pi f_c t) \quad (\text{sinc function}), \quad (11.2.10)$$

with signal-to-noise ratio (SNR) chosen so that the influence of $N(t)$ is small, and $B = \alpha T$, $BT \gg 1$, and $f_c = f_0$. Figure 11.6 shows the two signals and their energy spectra for an SNR equal to 16 dB; whereas Figure 11.7 shows similar results for an SNR equal to 8 dB. Although the two random signals are fundamentally different, their spectra are very similar. The information that separates the two signals is contained in the phase spectrum which is lost when we use the power spectral density (PSD) of the signals. To obtain the signal from the PSD we need to reconstruct the phase. The sinc and chirp functions have nearly identical magnitude spectra and in order to differentiate between the two we need to know their respective phases. The sinc function has zero phase (i.e., all frequencies arrive at once) while the chirp signal has the frequencies arriving in a certain order (phase is a quadratic function of time yielding a linear time-delay). Therefore, we see that there is a strong connection between the phase spectrum and TFDs. This

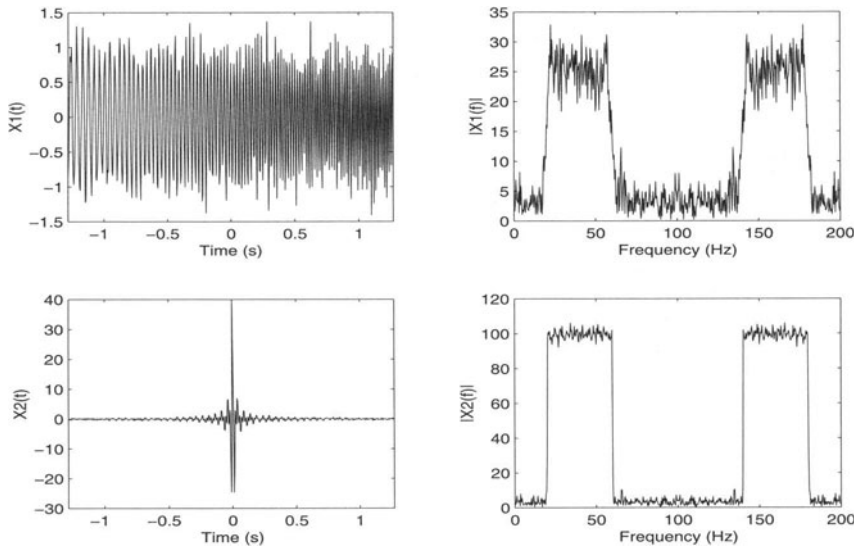


FIGURE 11.6. The top two plots show the chirp signal and its resulting energy spectrum for an SNR=16 dB. The bottom plots show the sinc function and its energy spectrum for the same SNR value.

is the group delay. The group delay gives the “order of arrival” of the frequencies. This observation leads us to define precisely the signal characteristics.

11.2.3 Signal characteristics

Important characteristics of a signal are:

- bandwidth, $B = f_{\max} - f_{\min}$;
- all frequencies that exist within B , from the smallest frequency f_{\min} to the largest frequency f_{\max} ;
- relative amplitude at these frequencies;
- the times at which these frequencies initially occur and remain present; and
- signal duration T .

All practical signals have a beginning and an end. T plays an equivalent role in time as B plays in frequency. For $0 < t < T$ we wish to know how the signal energy is distributed.

11.2.3.1 Instantaneous frequency (IF) and group delay

The IF of a signal $s(t) = a(t) \cos \phi(t)$ is given by

$$f_i(t) = \frac{1}{2\pi} \frac{d\phi(t)}{dt}. \quad (11.2.11)$$

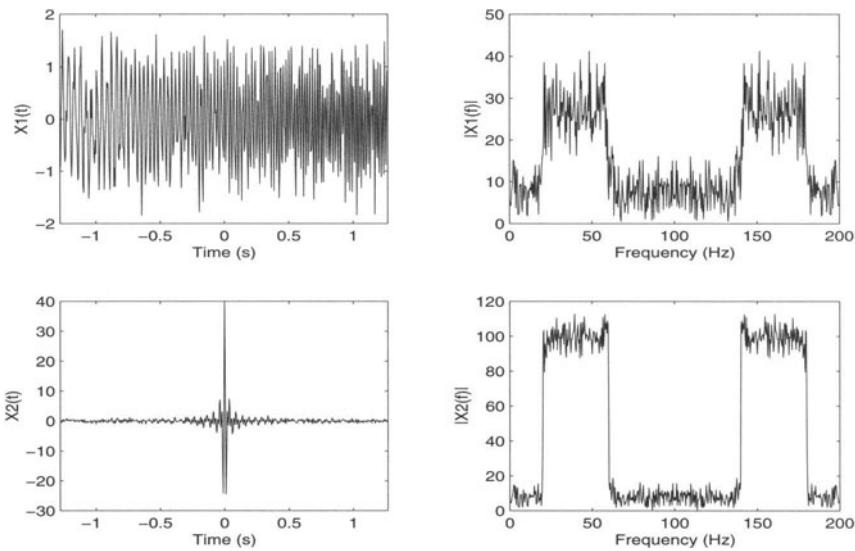


FIGURE 11.7. The top two plots show the chirp signal and its resulting energy spectrum for an SNR=8 dB. The bottom plots show the sinc function and its energy spectrum for the same SNR value.

To find the IF we use the analytic signal, $z(t)$, which is given by [3], [4]:

$$z(t) = s(t) + j\mathcal{H}\{s(t)\} \quad (11.2.12)$$

$$= a(t)e^{j\phi(t)} \quad (\text{under certain conditions that are met by asymptotic signals}). \quad (11.2.13)$$

where $\mathcal{H}[\cdot]$ refers to the Hilbert transform [4].

The “group delay” is defined as

$$\tau_g(f) = -\frac{1}{2\pi} \frac{d\theta(f)}{df}, \quad (11.2.14)$$

where

$$\mathcal{F}\{z(t)\} = Z(f) = A(f)e^{j\theta(f)}. \quad (11.2.15)$$

11.2.3.2 Duration-bandwidth product

A class of asymptotic signals was defined to satisfy the following [1]:

- finite energy;
- finite duration;
- bounded maximum amplitude; and
- BT large (> 10). This ensures that the error made in assuming a band and time-limited function is small.

The BT product represents the richness of information (number of degrees of freedom) in the signal [1]. For short signals, characterization of the signal by the IF has little meaning.

Finite Duration Signal.

A finite duration signal, $s_l(t)$, can be expressed as

$$s_l(t) = s(t) \operatorname{rect}\left(\frac{t}{T}\right) \quad (11.2.16)$$

where $\operatorname{rect}(t/T)$, a unit amplitude rectangular window of duration T and located at $t = 0$, expresses the fact that the signal is zero outside its duration, and the subscript l indicates the time *limited* nature of the signal.

The FT of the finite duration signal is

$$S_l(f) = S(f) *_f T \operatorname{sinc}(fT), \quad (11.2.17)$$

where $*_f$ defines the convolution operation in frequency.

Thus, the bandwidth of $S_l(f)$ is $B = \infty$. In some applications, a different window type, say $w(t)$, may be used instead of the rectangular window (for example, to reduce the effects of discontinuities). In this case, we can still write

$$s_l(t) = s(t) \operatorname{rect}\left(\frac{t}{T}\right) w(t). \quad (11.2.18)$$

Here again, the FT of the above expression shows that the bandwidth of $S_l(f)$ is still infinite. In order to have a limited bandwidth, we must choose $T = \infty$ (since, in this case, $T \operatorname{sinc}(fT) \rightarrow \delta(f)$), but in this situation we end up with an infinite duration signal.

The duration of a signal can be measured using the effective duration T_e given by

$$T_e^2 = \frac{\int_{-\infty}^{\infty} t^2 |s(t)|^2 dt}{\int_{-\infty}^{\infty} |s(t)|^2 dt}. \quad (11.2.19)$$

Finite Bandwidth Signal.

In analogy to the finite duration signal, we define the finite bandwidth signal as

$$S_l(f) = S(f) \cdot \operatorname{rect}\left(\frac{f}{B}\right). \quad (11.2.20)$$

The signal is then given by

$$s_l(t) = s(t) *_t B \operatorname{sinc}(Bt) \quad (11.2.21)$$

which has an infinite duration and all the above comments apply.

The bandwidth of a signal can be measured using the effective bandwidth B_e given by

$$B_e^2 = \frac{\int_{-\infty}^{\infty} f^2 |S(f)|^2 df}{\int_{-\infty}^{\infty} |S(f)|^2 df}. \quad (11.2.22)$$

Thus, for a given signal, a finite duration means an infinite bandwidth and a finite bandwidth means an infinite duration.

11.2.3.3 Relation between IF and group delay: An example

The signal, $s(t)$, is defined by

$$s(t) = \text{rect}\left(\frac{t}{T}\right) \cos \phi(t), \quad (11.2.23)$$

where

$$\phi(t) = 2\pi \left(f_c t + \frac{\alpha}{2} t^2 \right), \quad \alpha = \frac{B}{T} \quad \text{and} \quad BT \gg 1. \quad (11.2.24)$$

The analytic signal is

$$z(t) = \text{rect}\left(\frac{t}{T}\right) e^{j\phi(t)}. \quad (11.2.25)$$

The IF of the signal is then given by

$$f_i(t) = \frac{1}{2\pi} \frac{d\phi(t)}{dt} = f_c + \alpha t. \quad (11.2.26)$$

Extracting t as a function of $f_i(t)$ gives the inverse operator of the IF, $g(t) = f_i^{-1}(t)$:

$$g(t) = \alpha^{-1}(f_i(t) - f_c). \quad (11.2.27)$$

The FT of $z(t)$ is [1]:

$$Z(f) \approx \frac{1}{\sqrt{\alpha}} \text{rect}\left(\frac{f - f_c}{B}\right) e^{j\pi[1/4 - \alpha^{-1}(f - f_c)^2]}. \quad (11.2.28)$$

The time delay is then

$$\tau_g(f) = \alpha^{-1}(f - f_c). \quad (11.2.29)$$

In this case, the instantaneous frequency and the time delay are the inverse of each other. The IF and the group delay give information about the internal organization of the signal [1].

11.3 Review of Contributions to Time-Frequency Signal Analysis

11.3.1 The early theoretical contributions

11.3.1.1 Gabor's theory of communication

In 1946 Gabor [8] proposed a TFD for the purpose of studying the question of efficient signal transmission, as he was dissatisfied with the physical results obtained by using the FT. In particular, the time-frequency exclusivity of the FT did not fit

with his intuitive notions of a time-varying frequency as found in speech or music. He wanted to represent other signals, not just those limiting cases of a “sudden surge” (delta function) or an infinite duration sinusoidal wave. By studying the response of a bank of filters that were constrained in time and frequency, Gabor performed a time-frequency analysis. He indicated that the bank of filters would effectively divide the time-frequency plane into a series of rectangles. He further noted that the dimensions of these rectangles, *tuning width* \times *decay time*, must obey Heisenberg’s uncertainty principle which translates in Fourier analysis to

$$\Delta t \cdot \Delta f \geq \frac{1}{4\pi}, \quad (11.3.1)$$

where Δt and Δf are the equivalent duration and bandwidth of the signal [8]. Gabor showed this relationship to be “at the root of the fundamental principle of communication” [8], since it puts a lower limit on the minimum spread of a signal in time and frequency. The product value of $\Delta t \cdot \Delta f = 1/4\pi$ gives the minimum area unit in this time-frequency information diagram, which is obtained for a complex Gaussian signal.

Gabor’s representation divided the time-frequency plane into discrete rectangles of information called logons. Each logon was assigned a complex value, $c_{m,n}$, where m represents the time index and n the frequency index. The $c_{m,n}$ coefficients were weights in the expansion of a signal into a discrete set of shifted and modulated Gaussian windows, which may be expressed as

$$s(t) = \sum_{m=-\infty}^{\infty} \sum_{n=-\infty}^{\infty} c_{m,n} \psi(t; m, n), \quad (11.3.2)$$

where $\psi(t; m, n)$ are Gaussian functions centered about time, m , and frequency, n [8].

Kay and Lerner [25] extended Gabor’s work by removing the rectangular constraint on the shape of the elementary cells. Helstrom [26] generalized the expansion by replacing the discrete elementary cell weighting with a continuous function, $\xi(\tau, t, f)$. Wavelet theory was later developed as a further extension of Gabor’s work, but with each partition of the time-frequency plane varying so as to yield a constant Q filtering [27].

11.3.1.2 The spectrogram and sonograph

As introduced earlier, the spectrogram which originated from early speech analysis methods represents an intuitive approach to spectrum analysis of nonstationary processes. It represents a natural transition from stationary processing toward time-frequency analysis. In this method, a local power spectrum (or periodogram) is calculated from slices of the signal centered around the successive time points of interest, as follows:

$$\rho_{\text{spec}}(t, f) = |S(t, f)|^2 = \left| \int_{-\infty}^{\infty} s(\tau) h(t - \tau) e^{-j2\pi f \tau} d\tau \right|^2, \quad (11.3.3)$$

$h(t - \tau)$ is the even time-limiting analysis window, centered at $t = \tau$, and $S(t, f)$ is referred to as the short-time Fourier transform (STFT). The time-frequency character of the spectrogram is given by its display of the signal as a function of the frequency variable, f , and the window center time. This is a simple and robust method, and has consequently enjoyed continuing popularity. However, as indicated earlier, it has some inherent problems. The frequency resolution is dependent on the length of the analysis window and thus degrades significantly as the size of the window is reduced, due to the uncertainty relationships. The equivalent method of filter banks (sonograph) consists of taking the windowed transformation of the signal spectrum as follows:

$$\rho_{FB}(t, f) = |S(t, f)|^2 = \left| \int_{-\infty}^{\infty} S(\nu) H(f - \nu) e^{j2\pi\nu t} d\nu \right|^2. \quad (11.3.4)$$

These two representations become identical if $h(t)$ and $H(f)$ are an FT pair [18]. This indicates that there exists the same compromise for the time resolution; i.e., there is an inherent trade-off between time and frequency resolution. The spectrogram and sonograph are still among the most popular tools for TFSA, due to their robustness to noise, linearity property, ease of use, and interpretation.

Optimal Window Choice in the Spectrogram and Sonograph.

The primary purpose of the window in the STFT is to limit the extent of the sequence to be transformed so that the spectral characteristics are reasonably stationary over the duration of the window. The more rapidly the signal characteristics change, the shorter the window should be. This means the frequency resolution decreases. On the other hand, as the window length decreases, the ability to resolve changes with time increases. Consequently, the choice of the window length becomes a tradeoff between frequency and time resolution.

The optimal window length is affected by the FM law of the signal. For a linear FM signal, the optimal window is given by [1]: $\Delta = \sqrt{T/B}$ where T is the signal duration and B is the signal bandwidth. This result is generalized for any given FM signal (whose IF is $f_i(t)$) by [1]:

$$\Delta = \left| \frac{df_i(t)}{dt} \right|^{-1/2}. \quad (11.3.5)$$

The optimal window length in the STFT does not yield delta functions around the signal's IF. Moreover, the optimal STFT requires an a priori knowledge of $f_i(t)$ which can only be obtained after some form of time-frequency analysis. This limitation can be partly overcome by using the WVD defined in a forthcoming section.

Similarly, we can also optimize the window length for a sonograph. The optimal bandwidth of the band-pass filters is related to the group delay in the same way the optimal window length for the STFT is related to the IF.

11.3.1.3 Page's instantaneous power spectrum

Page [10] also proposed to extend the notion of power spectrum to deal with time-varying signals. He defined the “instantaneous power spectra” (IPS), $p(t, f)$, as the distribution, over both time and frequency, of the total signal energy, E_T , contained up to time T ; i.e.,

$$E_T = \int_{-\infty}^T \int_{-\infty}^{\infty} p(t, f) df dt. \quad (11.3.6)$$

It is a spectral representation of the signal, which varies as a function of time. In order to obtain an expression for $p(t, f)$, Page first defined a running transform

$$S^-(t, f) = \int_{-\infty}^t s(\tau) e^{-j2\pi f\tau} d\tau \quad (11.3.7)$$

which represents the conventional FT of the signal, but calculated only up to time t . He then defined his IPS as the rate of change or gradient in time of $S^-(t, f)$; i.e., the contribution to the overall energy made by each frequency component. This is defined as follows:

$$p(t, f) = \frac{\partial}{\partial t} |S^-(t, f)|^2. \quad (11.3.8)$$

It may equivalently be expressed as

$$p(t, f) = 2s(t)\mathcal{R}\{e^{j2\pi ft} S^-(t, f)\} \quad (11.3.9)$$

or

$$p(t, f) = 2 \int_0^{\infty} s(t)s(t - \tau) \cos 2\pi f\tau d\tau, \quad (11.3.10)$$

where $\mathcal{R}\{\cdot\}$ denotes the real part.

Since $p(t, f)$ is a gradient, it may contain negative values; it redistributes signal energy as time evolves, compensating for previous values which were either too low or too strong. The IPS therefore does not localize the information in time and frequency. Turner [11] has shown that the IPS is not unique, since any complementary function which integrates to zero in frequency can be added to it without changing the distribution. He also proved that the IPS is dependent on the initial time of observation. This indicates that the IPS is not a “true” TFD as it does not meet some of the requirements that a signal analyst expects in order to carry out a practical analysis of the signal. Nevertheless, it represented an important step in the development of ideas which led to our current understanding of TFDs. In particular, it provides for an interpretation of the negative values of TFDs.

Levin [12], following Page's work, defined a forward running (or anticausal) spectrum $S^+(t, f)$, which is based on future time values, by taking a FT from t to $+\infty$. He also defined a time-frequency representation taking an average of the forward and backward IPS to get

$$p_L(t, f) = \frac{1}{2} \left[\frac{\partial}{\partial t} |S^-(t, f)|^2 + \frac{\partial}{\partial t} |S^+(t, f)|^2 \right] \quad (11.3.11)$$

$$= 2s(t)\mathcal{R}\{e^{j2\pi f t}S(f)\}. \quad (11.3.12)$$

By realizing that this combination would lead to an overall time-frequency representation which would describe the signal in a better way, Levin defined a distribution that is very similar to Rihaczek's distribution [13] discussed below.

11.3.1.4 Rihaczek's complex energy density

Starting from physical considerations, Rihaczek formed a time-frequency energy density function for a complex deterministic signal, $z(t)$, which, he claimed, was a natural extension of the energy density spectrum, $|Z(f)|^2$, and the instantaneous power, $|z(t)|^2$. His reasoning was as follows:¹ the total energy of a complex signal, $z(t)$, is

$$E = \frac{1}{2} \int_{-\infty}^{\infty} |z(t)|^2 dt. \quad (11.3.13)$$

Consider a bandlimited portion of the original signal, around a central frequency f_c , $z_1(t)$ given as

$$z_1(t) = \mathcal{F}^{-1} \left\{ \text{rect} \left(\frac{f - f_c}{\Delta B} \right) \cdot Z(f) \right\}, \quad (11.3.14)$$

$z_1(t)$ contains the energy

$$E_1 = \frac{1}{2} \int_{-\infty}^{\infty} z(t)z_1^*(t) dt. \quad (11.3.15)$$

If the bandwidth of $z_1(t)$ is reduced ($\Delta B \rightarrow \delta B$), then $z_1(t) = Z(f_c)\delta B e^{-j2\pi f_c t}$ and we obtain

$$E_1 = \frac{1}{2} \int_{-\infty}^{\infty} z(t)Z^*(f_c)\delta B e^{-j2\pi f_c t} dt \quad (11.3.16)$$

assuming that $Z(f)$ is constant over the spectral band, δB , which is reasonable if $\delta B \rightarrow 0$.

The quantity in (11.3.16) represents the energy in a small spectral band, δB , but over all time. To obtain the energy within a small frequency band, δB , and a time band, ΔT , it suffices to limit the integration to ΔT , as follows:

$$E_1 = \frac{1}{2} \int_{-t_0 - \Delta T/2}^{t_0 + \Delta T/2} z(t)Z^*(f_c)\delta B e^{-j2\pi f_c t} dt. \quad (11.3.17)$$

Taking the limit $\Delta T \rightarrow \delta T$ yields

$$E_1 = \frac{1}{2} \delta B \delta T z(t_0) Z^*(f_c) e^{-j2\pi f_c t_0} \quad (11.3.18)$$

with the resultant time-frequency energy density function being

$$\rho_R(t, f) = z(t)Z^*(f)e^{-j2\pi f t} \quad (11.3.19)$$

¹Here we give a formal, although not strictly rigorous, derivation of the distribution.

which is generally referred to as the Rihaczek distribution (RD). If $z(t)$ is real, one can see that Levin's TFD (which is based on Page's TFD) is simply twice the real part of Rihaczek's TFD.

These different approaches to define a TFD are all natural and straightforward; yet, they seem to lead to different definitions of a TFD. In fact, all of them are related and fit within a general formula, called the quadratic class, described in later sections.

11.3.1.5 The Wigner–Ville distribution

Ville's work [9] followed Gabor's contribution; he also noted the insufficiency of time analysis and frequency analysis, using the same analogy of a piece of music. He indicated that since a signal has a spectral structure at any given time, there should exist the notion of an “instantaneous spectrum” which has the physical attributes of an energy density. Thus, the energy within a small portion of the time-frequency plane, $dt \cdot df$, would be

$$E_\delta = W(t, f) dt df \quad (11.3.20)$$

and its integration over f (respectively, over t) should yield the instantaneous energy $|s(t)|^2$ (respectively, the spectrum $|S(f)|^2$). Integration over both t and f would yield the energy, E :

$$\int_{-\infty}^{\infty} W(t, f) df = |s(t)|^2, \quad (11.3.21)$$

$$\int_{-\infty}^{\infty} W(t, f) dt = |S(f)|^2, \quad (11.3.22)$$

$$\int_{-\infty}^{\infty} \int_{-\infty}^{\infty} W(t, f) dt df = E. \quad (11.3.23)$$

These desirable properties led Ville to draw an analogy with the probability density function (pdf) of quantum mechanics by considering that:

1. the distribution to be found is equivalent to the joint pdf in time and frequency;
2. the instantaneous power is equivalent to one conditional probability (or marginal); and
3. the energy spectrum is equivalent to the other conditional probability (or marginal).

Then, one could form the characteristic function, $F(u, v)$, of this TFD, and equate the marginal results of $|s(t)|^2$ and $|S(f)|^2$ with the moments generated from the characteristic function (using its moment generating properties):

$$W(t, f) = \mathcal{F}_{i \rightarrow u} \mathcal{F}_{f \rightarrow v} F(u, v). \quad (11.3.24)$$

Using then the framework of quantum mechanical operator theory [28], Ville established that the proper form for the distribution was

$$W(t, f) = \int_{-\infty}^{+\infty} z\left(t + \frac{\tau}{2}\right) \cdot z^*\left(t - \frac{\tau}{2}\right) e^{-j2\pi f\tau} d\tau, \quad (11.3.25)$$

where $z(t)$ is the analytic complex signal which corresponds to the real signal, $s(t)$ [29] (see Section 11.2.3.1).

Ville's distribution was derived earlier by Wigner in a quantum mechanical context [30]. For this reason, it is generally referred to as the Wigner–Ville distribution (WVD) and it is the most widely studied TFD. The WVD has many desirable properties as a signal processing tool. It is a real joint distribution of the signal in time and frequency. The marginal distributions in time and frequency can be retrieved by integrating the WVD in frequency and time, respectively. It achieves maximum energy concentration in the time-frequency plane about the IF for linearly frequency modulated signals. It is also time-, frequency-, and scale-invariant, and so fits well into the framework of linear filtering theory. The disadvantages of the WVD are that it is nonpositive, it is bilinear, and it has cross-terms. The cross-terms cause “ghost” energy to appear midway between the true energy components. A detailed review of the WVD is provided in [1].

11.3.2 The second phase of advances in TFSA

11.3.2.1 Main developments in the 1980s

The early research in the 1980s focused on the WVD as engineers and scientists started to discover that it provides a means to attain good frequency localization for rapidly time-varying signals. For example, in a seismic context, it was shown to be a very effective tool to represent Vibroseis chirp signals emitted in seismic processing [31], and hence was used to control the quality of the signal emitted. When the signal emitted was a pure linear FM, the WVD exhibited a sharp peak along the FM law. This property was lost if the signal was contaminated by harmonic coupling effects and other distortions [32].

The interest in the WVD increased due to its good behavior on chirp signals, the rediscovery of its special properties which made it attractive for the analysis of time-varying signals, and the advance of digital computers which allowed the computation of the previously prohibitive two-dimensional distribution [20]. (To the authors' best knowledge, the first WVD programme was written by Boashash in APL language in September 1978, for the processing of Vibroseis chirp data [20]. The program is reprinted in [31].)

In 1978, Boashash recognized that the WVD of a signal, $z(t)$, could be conceived as the FT of a quadratic kernel [20], i.e.,

$$W_z(t, f) = \mathcal{F}_{\tau \rightarrow f} [K_z(t, \tau)], \quad (11.3.26)$$

where $\mathcal{F}_{\tau \rightarrow f}$ represents an FT with respect to the τ variable, and where $K_z(t, \tau)$ is the quadratic kernel defined by

$$K_z(t, \tau) = z \left(t + \frac{\tau}{2} \right) z^* \left(t - \frac{\tau}{2} \right). \quad (11.3.27)$$

Most of the early research in the WVD concentrated on the case of deterministic signals, for which the WVD is interpreted as a distribution of signal energy in the time-frequency (t-f) domain. For random signals, it was shown [33] that the expected value of the WVD equals the FT of the time-varying autocorrelation function (see section 11.4 for more details). This gave the WVD an important interpretation as a time-varying PSD and sparked significant research efforts along this direction.

Filtering and Signal Synthesis. It was also realized early that the WVD could be used as a time-varying filter [34]. A simple algorithm could mask (i.e., filter) sections of the time-frequency plane using the WVD of the input signal and then perform a least-squares inversion of the WVD to recover the filtered signal [1], [34]. It was also shown that the input-output convolution relationships of filters were preserved when one used the WVD to represent the signals.

Implementation. The computational properties of the WVD were further studied and this led to an efficient real-time implementation which exploits the symmetry properties of the WVD kernel $K_z(t, \tau)$ [35].

Signal Detection, Estimation, and Classification. The areas of detection and estimation saw significant theoretical developments based on the WVD, [36], [37], [38], motivated by the belief that signal characterization should be more accurate in a joint time-frequency domain. A key property helped motivate this interest: the WVD is a unitary (energy-preserving transformation). Therefore, many of the classical detection and estimation problem solutions had alternate implementations based on the WVD. The two-dimensional, time-frequency nature of the implementation, however, allowed greater flexibility than did the classical one [39], [40].

The theory and important properties of the WVD which prompted so much interest were reviewed in detail in [1].

A mistake that was made by many of the early researchers was to “sell” uninhibitedly the method as a universal tool, whereas its field of application is really quite specialized. As the WVD became increasingly exposed to the signal processing community, users started to discover the limitations of the method, which are presented below.

11.3.2.2 Limitations of the WVD

Nonlinearities. The WVD is nonlinear. It performs a quadratic transformation of the frequency components of a signal equivalent to a “dechirping” operation. For multicomponent signals, the quadratic nature of the WVD causes it to create cross-terms which occur in between individual components. This often makes the

WVD difficult to interpret, such as in cases where there are many components or where components are not well separated. In addition, the bilinearity exaggerates the effect of additive noise by creating cross-terms between the signal component and the noise component. At low SNR, where the noise dominates, this may lead to a very rapid degradation of performance, if not dealt with properly. Further, even for monocomponent signals, artifacts are created in the case of nonlinear FM signals. Such problems are remedied by methods presented in next section.

Limited Duration. Another drawback sometimes attributed to the WVD is that it performs well only for infinite duration signals. Real-life signals, however, are time limited, therefore there is a need to take a windowed FT of the quadratic kernel [35], [41], [42].

Cross WVD (XWVD). An approach to reduce or nullify the presence of cross-terms was based on replacing the WVD by the XWVD in order to obtain a distribution which is linear in the signal. The XWVD could be interpreted as an extension of the cross-correlation function for nonstationary signals. The XWVD is defined as

$$W_{12}(t, f) = \mathcal{F}_{\tau \rightarrow f} [K_{12}(t, \tau)], \quad (11.3.28)$$

where

$$K_{12}(t, \tau) = z_1 \left(t + \frac{\tau}{2} \right) z_2^* \left(t - \frac{\tau}{2} \right), \quad (11.3.29)$$

where $z_1(t)$ is a reference signal and $z_2(t)$ is the signal under analysis. There were then systematic efforts in trying to substitute the use of the XWVD in all areas of application of the WVD. In many cases, this was straightforward, because a reference signal, as well as an observed signal, was available. Thus, the XWVD was proposed for optimal detection schemes [36], for sonar and radar applications [43], and for seismic exploration [44]. These schemes were seen to be equivalent to traditional matched filter and ambiguity function-based schemes, but their representation in another domain allowed for some flexibility and variation. In other cases, where reference signals were not available, the XWVD could not easily be applied, a fact which often prevented the further spread of the XWVD as a replacement for the WVD.

In some applications, however, it is possible to define reference signals from filtered estimates of the original signal, and then use it as if it were the true signal. The filtering procedure often uses the IF as a critical feature of the signal. Jones and Parks [45] implicitly used a similar philosophy to estimate their data-dependent distributions. They estimated their reference signal as that signal component which maximized the energy concentration in the distribution.

Wideband TFDs. The problems relating to the WVD's reduced performance with short duration or wideband signals were addressed in several ways, such as using autoregressive modeling techniques. Attention was also given to designing wideband or *affine* time-frequency representations. The first to be considered was the wavelet transform, which is linear. It was like the Gabor transform in that it obtained its coefficients by projecting the signal onto basis functions corresponding

to different positions in time-frequency. The wavelet transform differed from the Gabor transform in that its basis functions all had the same shape. They were simply dilated (or scaled) and time-shifted versions of a *mother* wavelet. This feature causes the representation to exhibit a *constant Q* filtering characteristic. That is, at high frequencies the resolution in time is good, while the resolution in frequency is poor. At low frequencies, the converse is true. Consequently, abrupt or step changes in time may be detected or analyzed very well.

Subsequent efforts aimed at incorporating these wideband analysis techniques to quadratic TFDs. One of the early attempts used the Mellin transform (rather than the FT) to analyze the quadratic kernel [46]. The Mellin transform is a scale-invariant transform, and as a consequence, is suited to constant *Q* analysis. An application of group theory led to the definition of a general quadratic class of scale-invariant TFDs [47]. Others showed that this class of TFDs could be considered to be smoothed (in the affine sense) WVDs [48]. These techniques were extended for use in wideband sonar detection applications [49], and in speech recognition [50].

11.4 Quadratic Time-Frequency Distributions

11.4.1 A derivation procedure

In this section, we derive (formally but not strictly rigorously) a general form of the quadratic class of time-frequency distributions. Consider a real random signal $x(t)$ (formed, for example, by the sum of a deterministic signal $s(t)$ and additive noise). Let us define $z(t)$ as the analytic signal associated with $x(t)$. The auto-correlation function of the complex random signal $z(t)$ is defined as

$$R_z(t_1, t_2) = E\{z(t_1) \cdot z^*(t_2)\}. \quad (11.4.1)$$

Let us introduce the variable τ such that $t_1 = t + \tau/2$ and $t_2 = t - \tau/2$. Then,

$$R_z(t, \tau) \stackrel{\Delta}{=} R_z(t_1, t_2) = E\left\{z\left(t + \frac{\tau}{2}\right) z^*\left(t - \frac{\tau}{2}\right)\right\}. \quad (11.4.2)$$

If the random signal $z(t)$ is stationary, then $R_z(t, \tau) = R_z(\tau)$. If the random signal $z(t)$ is not stationary, then $R_z(\tau)$ can only provide a rough approximation to the true auto-correlation, $R_z(t, \tau)$.

The PSD of $z(t)$ is given by the application of the Wiener–Khintchine theorem,

$$R_z(t, \tau) \longleftrightarrow_f S_z(t, f) = \int_{-\infty}^{\infty} E\left\{z\left(t + \frac{\tau}{2}\right) z^*\left(t - \frac{\tau}{2}\right)\right\} e^{-j2\pi f \tau} d\tau. \quad (11.4.3)$$

Under some regularity assumptions, met by a large class of real-life signals, it follows that

$$\begin{aligned} S_z(t, f) &= E\left\{\int_{-\infty}^{\infty} z\left(t + \frac{\tau}{2}\right) z^*\left(t - \frac{\tau}{2}\right) e^{-j2\pi f \tau} d\tau\right\} \\ &= E\{W_z(t, f)\}. \end{aligned} \quad (11.4.4)$$

If $z(t)$ is deterministic, we can write

$$S_z(t, f) = W_z(t, f) \quad (11.4.5)$$

$$= \tau \xrightarrow{\mathcal{F}} f \quad \left[z\left(t + \frac{\tau}{2}\right) z^*\left(t - \frac{\tau}{2}\right) \right]. \quad (11.4.6)$$

In practice, we only have a finite duration signal. In other words, a windowed version of the above bilinear kernel is considered. Thus, we have $g_1(\tau)z(t+\tau/2)z^*(t-\tau/2)$ where $g_1(t)$ is a finite length window (defined as the effective analysis window in [1, p. 457]). The same remark can be made for the frequency range.

Therefore, in practice, the time-varying spectrum is obtained as

$$\hat{S}_z(t, f) = W_z(t, f) *_f G_1(f) *_t g_2(t), \quad (11.4.7)$$

where $G_1(f) = \mathcal{F}\{g_1(\tau)\}$ is due to the signal finite duration and $g_2(t) = \mathcal{F}^{-1}\{G_2(f)\}$ is due to the signal finite bandwidth. The estimated time-frequency representation is then

$$\hat{S}_z(t, f) = W_z(t, f) * * \gamma(t, f), \quad (11.4.8)$$

where $\gamma(t, f) = G_1(f)g_2(t)$ and the double asterisk indicates convolution in both time and frequency.

If one then decides to vary $\gamma(t, f)$ according to some criteria so as to refine some measurement, one obtains a general TFD which could adapt to the signal characteristics. These characteristics may be inherent to the signal or may be caused by the observation process. If we write the double convolution in full, we obtain

$$\rho(t, f) = \int_{-\infty}^{\infty} \int_{-\infty}^{\infty} \int_{-\infty}^{\infty} e^{j2\pi\nu(u-t)} g(\nu, \tau) z\left(u + \frac{\tau}{2}\right) \cdot z^*\left(u - \frac{\tau}{2}\right) e^{-j2\pi f\tau} d\nu du d\tau. \quad (11.4.9)$$

This formula was used in [51] in quantum mechanics. Note that $g(\nu, \tau)$, called the kernel function, is related to $\gamma(t, f)$ by the double FT: $\gamma(t, f) = \underset{\nu \rightarrow t}{\mathcal{F}} \underset{\tau \rightarrow f}{\mathcal{F}^{-1}} [g(\nu, \tau)]$. By varying the kernel $g(\nu, \tau)$, we can recover all the TFDs presented in Section 11.3.

11.4.2 Time, frequency, lag, and Doppler representations of the quadratic class of TFDs

In the following, we show that a nonstationary signal can be analyzed in four different domains. All these domains are related to one another by one- or two-dimensional FTs and the design of a quadratic TFD could be performed in any one of them.

11.4.2.1 Relationship between quadratic TFDs and the ambiguity domain

Equation (11.4.9) can be rewritten as the two-dimensional FT of the generalized ambiguity function, i.e.,

$$\rho_z(t, f) = \int_{-\infty}^{+\infty} \int_{-\infty}^{+\infty} \mathcal{A}_z(\nu, \tau) e^{-j2\pi\nu t - j2\pi f\tau} d\nu d\tau \quad (11.4.10)$$

with

$$\mathcal{A}_z(\nu, \tau) = g(\nu, \tau) \cdot A_z(\nu, \tau), \quad (11.4.11)$$

where $A_z(\nu, \tau)$ is the Sussman ambiguity function (a.k.a. the symmetrical ambiguity function) given by

$$A_z(\nu, \tau) = \int_{-\infty}^{+\infty} z(u + 0.5\tau)z^*(u - 0.5\tau)e^{j2\pi\nu u} du. \quad (11.4.12)$$

The previous expressions show that the TFD, $\rho_z(t, f)$, is equivalent to a two-dimensional filtering in the ambiguity domain (also called Doppler-lag domain) (ν, τ) .

11.4.2.2 Relationship between quadratic TFDs and the time-lag domain

By taking the inverse FT of the kernel function with respect to ν , we obtain

$$G(t, \tau) = \int_{-\infty}^{+\infty} g(\nu, \tau)e^{+j2\pi\nu t} d\nu \quad (11.4.13)$$

leading to

$$G(u - t, \tau) = \int_{-\infty}^{+\infty} g(\nu, \tau)e^{+j2\pi\nu(u-t)} d\nu. \quad (11.4.14)$$

We can easily see that (11.4.9) can be rewritten as

$$\rho_z(t, f) = \int_{-\infty}^{+\infty} \int_{-\infty}^{+\infty} G(u - t, \tau)z(u + 0.5\tau)z^*(u - 0.5\tau)e^{-j2\pi f \tau} du d\tau. \quad (11.4.15)$$

For most TFDs, the kernel, $g(\nu, \tau)$, is chosen in the (ν, τ) domain (Doppler-lag domain) and its implementation is performed in the (t, τ) domain (time-lag domain). If the function $G(t, \tau)$ is symmetrical about t , the expression of $\rho_z(t, f)$ reduces to

$$\rho_z(t, f) = \mathcal{F}_{\tau \rightarrow f}[G(t, \tau) *_t K_z(t, \tau)], \quad (11.4.16)$$

where $*_t$ means the convolution operation in time t and $K_z(t, \tau) = z(t + 0.5\tau)z^*(t - 0.5\tau)$.

11.4.2.3 Relationship between quadratic TFDs and the Doppler-frequency domain

The Doppler-frequency domain formulation of quadratic TFDs is given by [1]:

$$\rho_z(t, f) = \int_{-\infty}^{\infty} \int_{-\infty}^{\infty} \Gamma(\nu, f - \eta)Z\left(\eta + \frac{\nu}{2}\right) \cdot Z^*\left(\eta - \frac{\nu}{2}\right) e^{j2\pi\nu t} d\eta d\nu, \quad (11.4.17)$$

where $Z(f)$ is the FT of the signal $z(t)$ and $\Gamma(\nu, f)$ is the two-dimensional FT of $G(t, \tau)$.

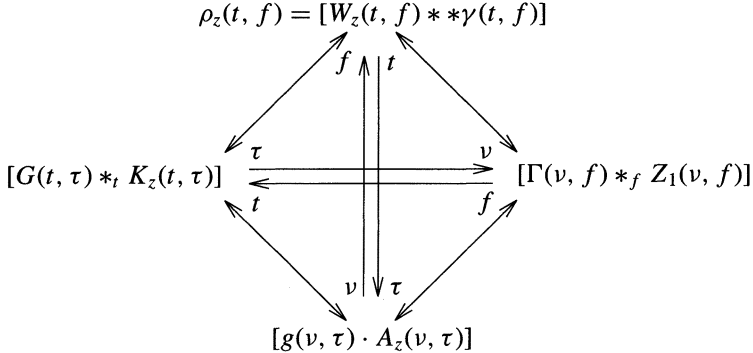


FIGURE 11.8. Nonstationary signals representations in four different domains.

Thus, we see that there are four possible domains for representing a non-stationary signal, namely, the time-frequency domain, the time-lag domain, the Doppler-lag domain, and the Doppler-frequency domain. All these domains are related to one another as shown in Figure 11.8. In this figure, $K_z(t, \tau) = z(t + 0.5\tau)z^*(t - 0.5\tau)$ and $Z_1(v, f) = Z(f + v/2) \cdot Z^*(f - v/2)$.

It was shown in the 1980s that nearly all the then known quadratic TFDs were obtainable from (11.4.9) by an appropriate choice of the kernel function $g(v, \tau)$. Most of the TFDs proposed since then are also members of the quadratic class. Some of those TFDs were discussed earlier. Others have been studied in detail and compared together in [1] and [2]. Table 11.1 lists some TFDs belonging to the quadratic class.

11.4.3 Multicomponent signal analysis

Since quadratic TFDs are a smoothed version of the FT of the quadratic kernel, $K_z(t, \tau)$:

$$K_z(t, \tau) = z\left(t + \frac{\tau}{2}\right) \cdot z^*\left(t - \frac{\tau}{2}\right) \quad (11.4.18)$$

there always exist cross-terms which are created in the TFD as a consequence of the interaction of different components of the signal. Consider a signal composed of two complex linear FM signal components

$$z_3(t) = z_1(t) + z_2(t). \quad (11.4.19)$$

The quadratic kernel of the signal $z_3(t)$ is

$$K_{z_3}(t, \tau) = K_{z_1}(t, \tau) + K_{z_2}(t, \tau) + K_{z_1 z_2}(t, \tau) + K_{z_2 z_1}(t, \tau), \quad (11.4.20)$$

where the cross-kernels, $K_{z_1 z_2}(t, \tau)$ and $K_{z_2 z_1}(t, \tau)$, are defined, respectively, by

$$K_{z_1 z_2}(t, \tau) = z_1\left(t + \frac{\tau}{2}\right) \cdot z_2^*\left(t - \frac{\tau}{2}\right), \quad (11.4.21)$$

$$K_{z_2 z_1}(t, \tau) = z_2\left(t + \frac{\tau}{2}\right) \cdot z_1^*\left(t - \frac{\tau}{2}\right). \quad (11.4.22)$$

TABLE 11.1. Some quadratic TFDs and their kernel functions $g(v, \tau)$.

Name	Kernel $g(v, \tau)$	Time-frequency distribution
WVD	1	$\int_{-\infty}^{\infty} z(t + 0.5\tau) z^*(t - 0.5\tau) e^{-j2\pi f \tau} d\tau$
Born-Jordan	$\frac{\sin \pi v \tau}{\pi v \tau}$	$\int_{-\infty}^{\infty} \frac{1}{\tau} e^{\int_{t-\tau/2}^{t+\tau/2} z(u + 0.5\tau) e^{-j2\pi f \tau} \times z^*(u - 0.5\tau) du} d\tau$
Rihaczek-Margenau		$\text{Re}[z(t)] Z^*(f) \cdot e^{-j2\pi f t} \}$
Page	$e^{j2\pi v \tau }$	$\frac{\partial}{\partial t} \left \int_{-\infty}^t z^{(u)} \cdot e^{-j2\pi f u} du \right ^2$
Spectrogram	$\int_{-\infty}^{\infty} h(u) \times \bar{h}^*(u - 0.5\tau) du$	$\left \int_{-\infty}^{\infty} s(\tau) h(t - \tau) d\tau \right ^2$
Choi-Williams	$e^{-4\pi^2 v^2 \tau^2 / \sigma}$	$\iint \frac{\sqrt{\sigma}}{\sqrt{4\pi \tau^2}} e^{-\sigma \frac{(u-t)^2}{4\tau^2} - j2\pi f t} z(u + 0.5\tau) \times z^*(u - 0.5\tau) du d\tau$
B-distribution	$ \tau ^{\sigma} \frac{2^{2\sigma-1}}{\Gamma(2\sigma)} \Gamma(\sigma + j\pi v) \Gamma(\sigma - j\pi v)$	$\iint \frac{ \tau ^{\sigma}}{\cosh^{2\sigma}(u-i)} e^{-j2\pi f \tau} z(u + 0.5\tau) \times z^*(u - 0.5\tau) du d\tau$

The third and fourth kernel terms comprise the cross-terms, which often manifest in the time-frequency representation in a confusing way. Consider the WVD of the signal consisting of two linear FM components, given in Figure 11.9. It shows three components, when one expects to find only two. The component in the middle exhibits large (positive and negative) amplitude terms in between the linear FMs signal energies where it is expected that there should be no energy at all. These are the cross-terms resulting from the quadratic nature of the TFD, which are often considered to be the fundamental limitations which have prevented more widespread use of TFSA. Some TFDs are able to reduce the magnitude of

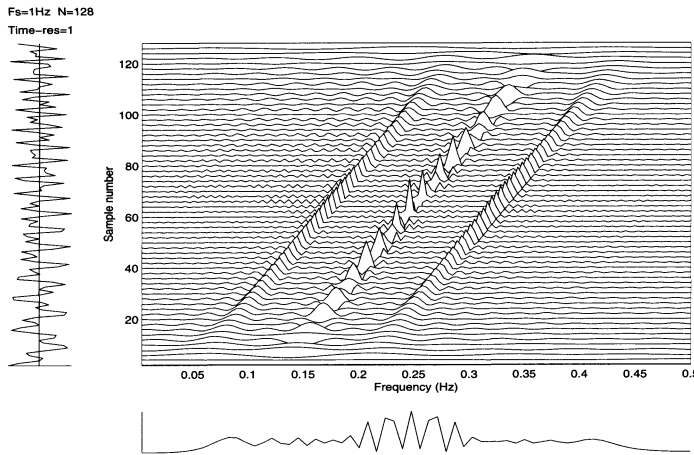


FIGURE 11.9. The WVD of a two-component signal formed by summing two linear FM signals.

the cross-terms, but they inevitably compromise some of the other properties of TFDs, such as resolution. One such a distribution is the “masked WVD” which has the advantages of both the WVD and the spectrogram while avoiding their drawbacks [52]; it is cross-terms free but has a high time-frequency resolution. It is obtained by taking the spectrogram as a mask for the WVD of the multicomponent signal. Thus, the resulting TFDs would be nonzero only in regions of the time-frequency plane at or near the auto-terms of the input signal.

As an example, consider the multicomponent signal consisting of two quadratic FM signals. Figures 11.10(a) and (b) display the WVD and the spectrogram of this signal. Figure 11.10(c) displays the resulting TFDs (the masked WVD). Note the elimination of the cross-terms compared to the WVD and the better resolution compared to the spectrogram. In Figure 11.11, we plot slices of the above distributions, with normalized amplitudes, to further illustrate the point.

The idea of masking was also used in [53] where the spectrogram was used in the threshold only (to decide for the on/off of the windowing), and where the resulting distribution is taken equal to the WVD in the case where the window is on. However, in our case, there is no thresholding consideration, and the resulting TFD is the product of the spectrogram with the WVD in the time-frequency domain.

11.4.3.1 Ambiguity domain filtering

Many researchers turned to two-dimensional Gaussian smoothing functions to reduce the cross-terms [46], [54], because of the Gaussian window property of minimizing the bandwidth-time product.

A key development, in a more effective effort at trying to reduce cross-terms, was to correlate this problem with a result from radar theory using the fact that in the ambiguity domain, the cross-terms tend to be distant from the origin, while the auto-terms are concentrated around the origin [55], [34]. Understanding this link

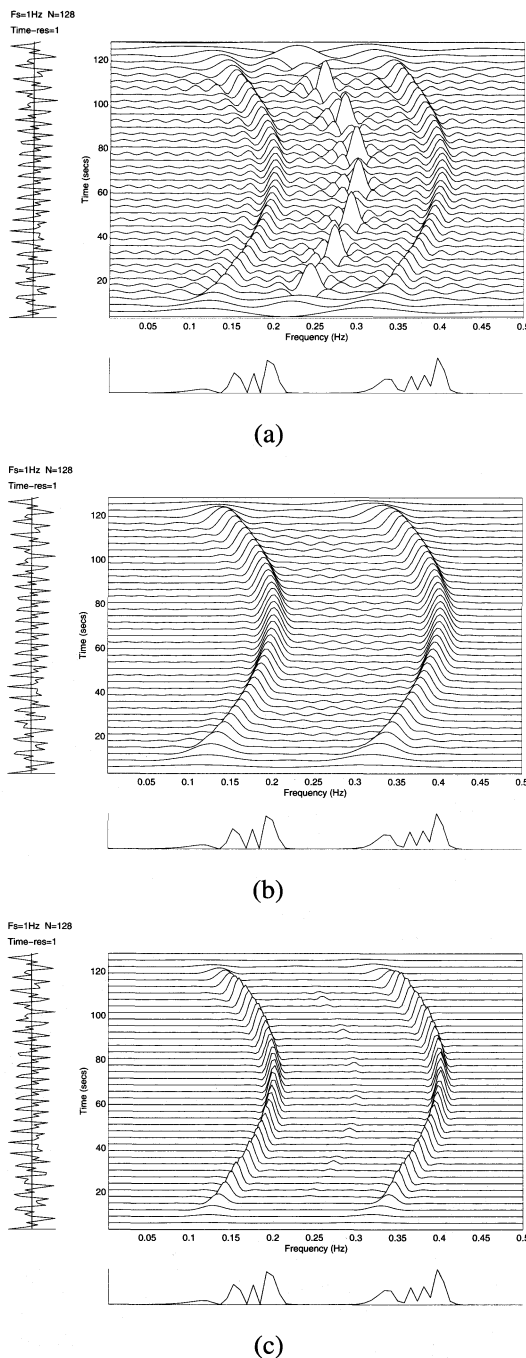


FIGURE 11.10. (a) The WVD, (b) the spectrogram, and the (c) masked WVD of a multicomponent signal consisting of two quadratic FM signals.

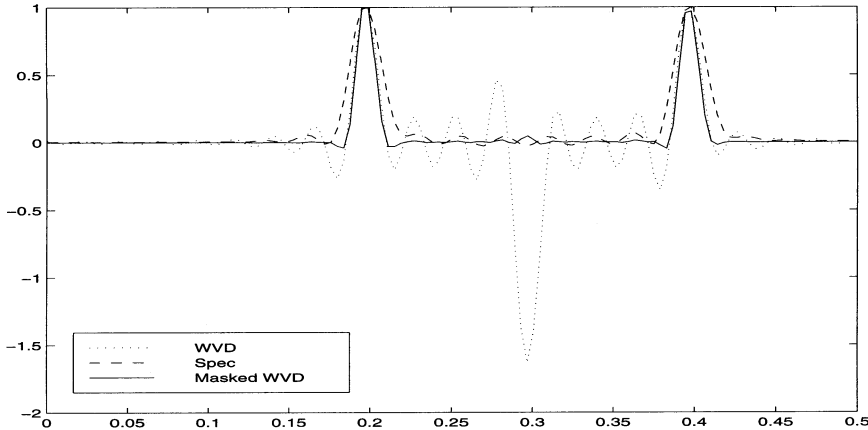


FIGURE 11.11. Slices of the normalized amplitudes of the WVD, the spectrogram, and the masked WVD at a certain time displayed in Figure 11.10. The x -axis represents the normalized frequency and the y -axis represents the normalized amplitudes.

was very helpful since the WVD was known to be related to the ambiguity function via a two-dimensional FT [1]. The natural way of reducing the cross-terms of the WVD was then simply to filter them out in the ambiguity domain, followed by a two-dimensional FT inversion.

This led to greater refinements and thought in the design of TFDs. Using this approach, TFDs can be designed with a variable level smoothing function, so that the artifacts could be reduced more or less depending on the application [56]. Other designed smoothing functions in which the artifacts folded back onto the auto-terms [57], [58], [59]. These authors showed how one could vary the shape of the cross-terms by an appropriate design of the smoothing function. Making the smoothing function data-dependent produced a signal-dependent TFD which achieved high energy concentration in the time-frequency plane [60]. This method was further refined using a signal-dependent TFD with a criterion of local adaptation [61] [62]. The cross-terms phenomenon is discussed in more detail in [1] and [2]. In the next section, we present a new TFD that provides a good time-frequency resolution in the analysis of multicomponent signals.

11.4.3.2 The B-distribution

As was stated earlier, there exist many TFDs and the use of a specific one depends on the desirable properties the representation should satisfy for that particular application. In most applications dealing with multicomponent signals, the analyst should be able to:

- know the number of components present in the signal;
- discriminate between the components and the existing cross-terms;
- resolve components that are close in the time-frequency plane; and

- estimate the instantaneous frequency of each component of the signal.

These points require that the TFD used in the analysis should be cross-terms free and should have high resolution in the time-frequency domain. Unfortunately, these two conditions seem to be mutually exclusive. And an intensive research effort has been deployed to design a TFD that satisfies both conditions simultaneously.

The B-distribution, a recently proposed TFD [63], is the closest to the ideal distribution; it is essentially cross-terms free and has high resolution in the time-frequency plane. We show, using synthetic and real-life data, that this proposed TFD outperforms the spectrogram and other existing reduced interference distributions in the analysis of multicomponent signals. In addition to that, we show that the B-distribution is practically equivalent to the WVD in the analysis and estimation of a monocomponent linear FM signal (recall that the WVD is optimal and efficient in the analysis of a linear FM signal [64]).

We define the time-lag kernel of the B-distribution as

$$G(t, \tau) = \left(\frac{|\tau|}{\cosh^2(t)} \right)^\sigma, \quad (11.4.23)$$

where σ is a real number that controls the sharpness of cut-off of the two-dimensional filter, in the ambiguity domain, resulting in a trade-off between time-frequency resolution and the elimination of cross-terms. The choice of σ is application-dependent; however, we have found that its range should be between zero and unity ($0 < \sigma \leq 1$). Extensive simulations and real-life data analysis show that $\sigma = 0.01$ gives the best results. But we stress that this value is not optimal for all situations and the analyst should choose the appropriate value for a given application.

The Doppler-lag domain representation of the B-distribution kernel is obtained by taking the FT of the time-lag kernel in (11.4.23) with respect to time t . That is,

$$g(\nu, \tau) = \int_{-\infty}^{+\infty} G(t, \tau) e^{-j2\pi\nu t} dt. \quad (11.4.24)$$

This results in

$$g(\nu, \tau) = |\tau|^\sigma \frac{2^{2\sigma-1}}{\Gamma(2\sigma)} \Gamma(\sigma + j\pi\nu) \Gamma(\sigma - j\pi\nu). \quad (11.4.25)$$

We can easily show that the B-distribution satisfies most of the important properties sought in a TFD [21], [1]. In particular:

- The B-distribution is real since $g(\nu, \tau) = g^*(-\nu, -\tau)$.
- The B-distribution is time-shift invariant since the Doppler-lag kernel is not a function of time t .
- The B-distribution is frequency-shift invariant since the Doppler-lag kernel is not a function of frequency f .

- The first moment of the B-distribution yields the instantaneous frequency of the signal under consideration. That is,

$$f_i(t) = \frac{\int_{-\infty}^{\infty} f \rho_z(t, f) df}{\int_{-\infty}^{\infty} \rho_z(t, f) df}. \quad (11.4.26)$$

This property is satisfied because [65], [1]:

$$\begin{cases} \frac{\partial g(\nu, \tau)}{\partial \tau}|_{(0,0)} = \frac{\partial g(\nu, \tau)}{\partial \nu}|_{(0,0)} = 0, \\ g(\nu, 0) = \text{constant for all } \nu. \end{cases} \quad (11.4.27)$$

11.4.3.3 Comparison of the B-distribution with other time-frequency distributions

In this section, we present several examples, using both synthetic and real data, to demonstrate the performance of the B-distribution and show its superiority over other TFDs in terms of cross-terms suppression and time-frequency resolution.

Two Parallel Signals. We consider the analysis of a multicomponent signal consisting of two linear FM signals that are parallel and close in the time-frequency domain. As we stated earlier, the WVD of such a signal will have cross-terms lying in between the two linear FM signals. It is known that in this case the use of a windowed WVD results in less cross-terms at the expense of resolution. In Figure 11.12, we plot the WVD, the Choi–Williams distribution (with the smoothing factor $\sigma = 1$), the Zhao–Atlas–Marks distribution (with the smoothing factor $a = 1$), the spectrogram, and the B-distribution. The window length was chosen equal to 31. The superiority of the B-distribution in resolving the two components, as well as reducing the cross-terms over the other TFDs, is very apparent. Other window lengths have also been used giving similar results. The analysis of two close parallel quadratic FM signals yields the same results as shown in Figure 11.13.

Automotive Signal. In this example, we analyze an automotive signal, namely, the cylinder pressure signal. This signal was collected using an in-cylinder pressure sensor that was mounted in the vicinity of the combustion chamber [66]. As in the previous example, a number of TFDs have been used for the purpose of comparison in the analysis of this signal. Figure 11.14 displays the windowed WVD, the Choi–Williams distribution ($\sigma = 1$), the Zhao–Atlas–Marks distribution ($a = 1$), the spectrogram, and the B-distribution of the automotive signal. Here again, we can see that the B-distribution outperforms the other distributions in providing high resolution while reducing the cross-terms between components.

Passive Acoustic Signal. In this last example, we consider another real-life problem to demonstrate the superiority of the B-distribution. The signal considered here is a real-life acoustic signal emitted from an overflying aircraft recorded and collected, under accurately monitored conditions, by a single ground-based microphone. This signal has been used to estimate the aircraft's flight parameters,

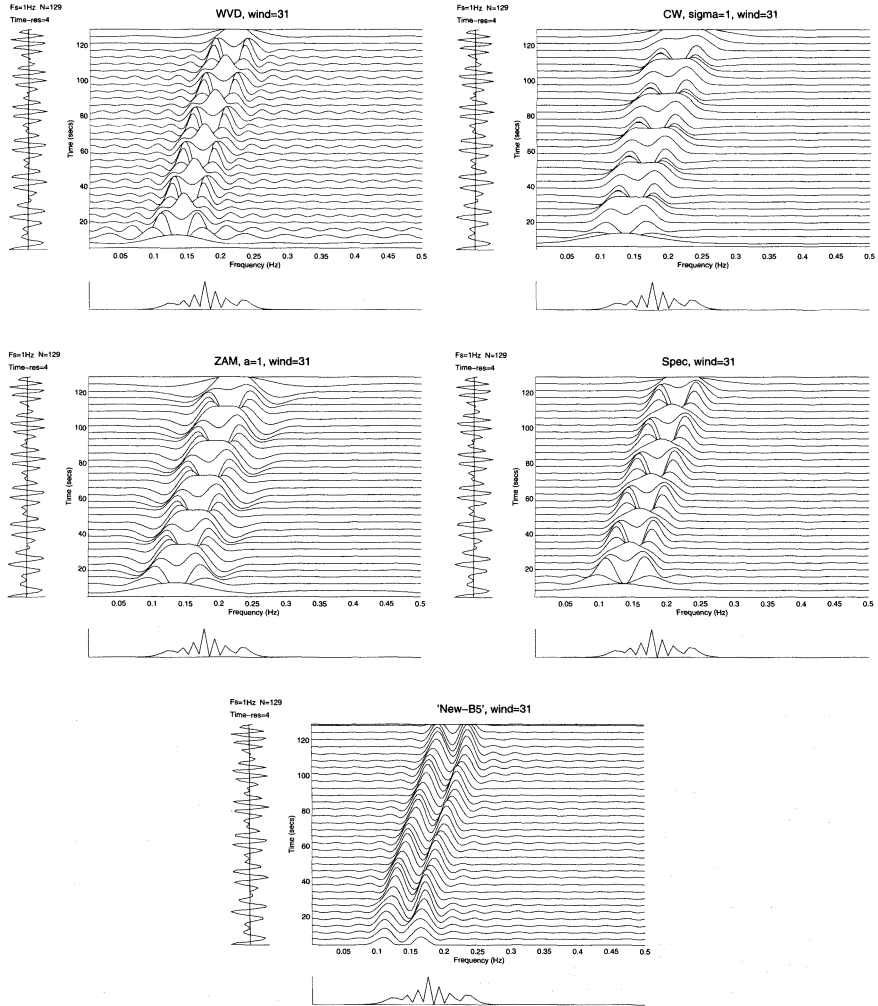


FIGURE 11.12. TFDs of a multicomponent signal consisting of two closely spaced linear FM signals. The WVD (top left), the Choi-Williams distribution (top right), the Zhao-Atlas-Marks distribution (center left), the spectrogram (center right), and the B-distribution (bottom).

namely, constant height, constant ground speed, constant acoustic frequency, and range [67]. Figure 11.15 displays the windowed WVD, the Choi-Williams distribution ($\sigma = 1$), the Zhao-Atlas-Marks distribution ($a = 1$), the spectrogram, and the B-distribution for the overflying aircraft signal. The superior performance of the B-distribution is evident.

From these examples, we see that the B-distribution is a very powerful tool for the analysis of multicomponent signals. This distribution is shown to solve problems

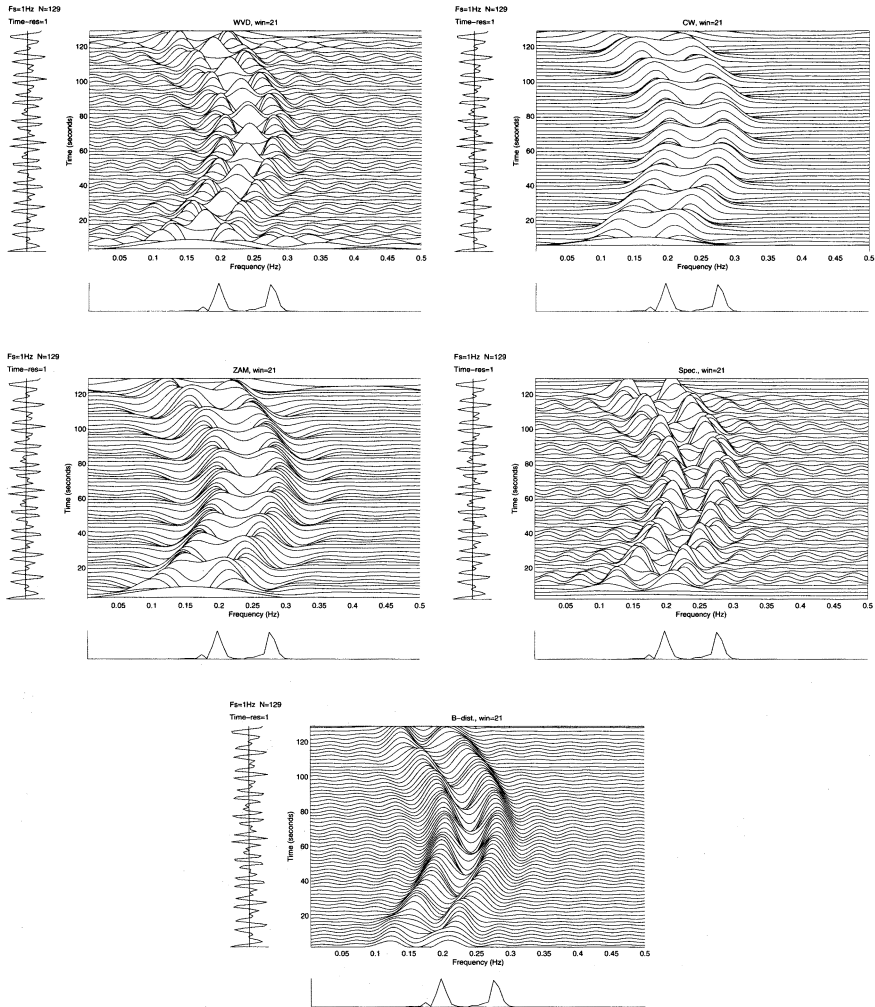


FIGURE 11.13. TFDs of a multicomponent signal consisting of two quadratic FM signals. The WVD (top left), the Choi–Williams distribution (top right), the Zhao–Atlas–Marks distribution (center left), the spectrogram (center right) and the B-distribution (bottom).

in situations where other existing distributions fail. For monocomponent signals (see the last example), the B-distribution is also very powerful and outperforms the spectrogram and the other reduced interference distributions.

Note. Here, there is no need to compare the B-distribution with the masked WVD (designed from the WVD and the spectrogram) since both the WVD and the spectrogram are shown to be inferior to the B-distribution.

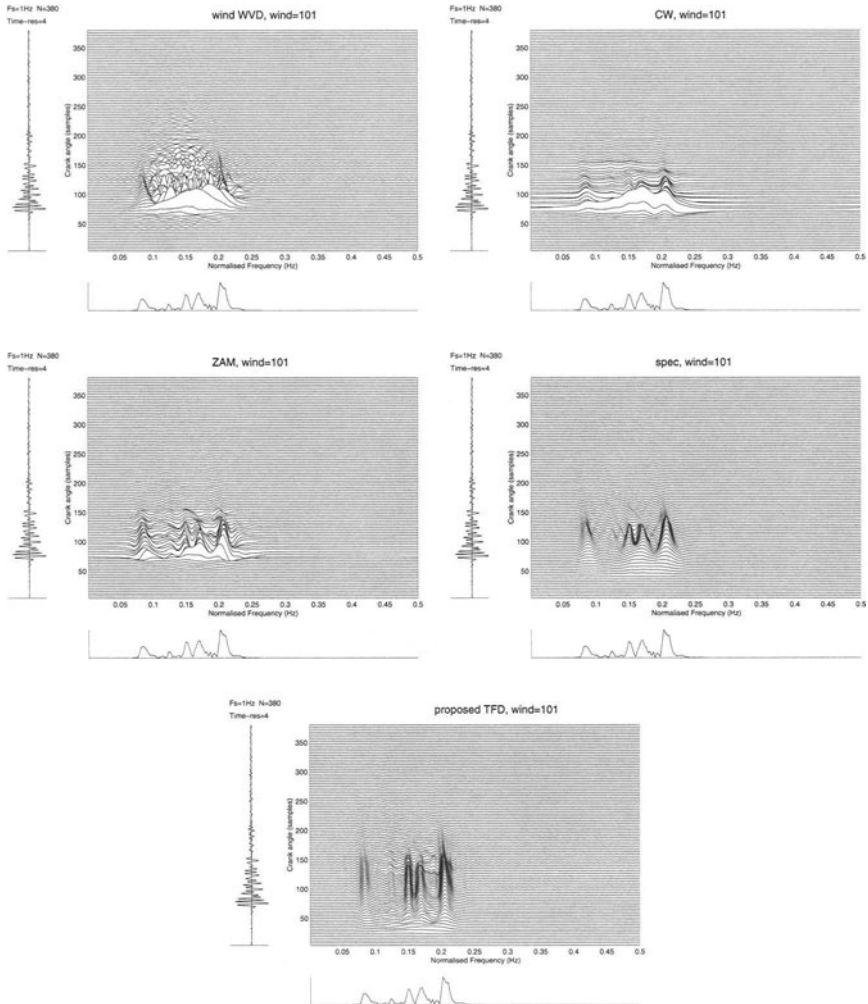


FIGURE 11.14. TFDs of a real-life multicomponent signal extracted from an automotive analysis. The WVD (top left), the Choi–Williams distribution (top right), the Zhao–Atlas–Marks distribution (center left), the spectrogram (center right), and the B-distribution (bottom).

11.4.3.4 Performance of the B-distribution for IF estimation of linear FM signals

In this section, we compare the B-distribution with the WVD in terms of the representation and estimation of a linear FM signal.

We already noted that the WVD is known to be optimal for linear FM signals. That is, the WVD yields delta functions around the instantaneous frequency of such signals [1]. For this reason, it was suggested using the peak of the WVD as

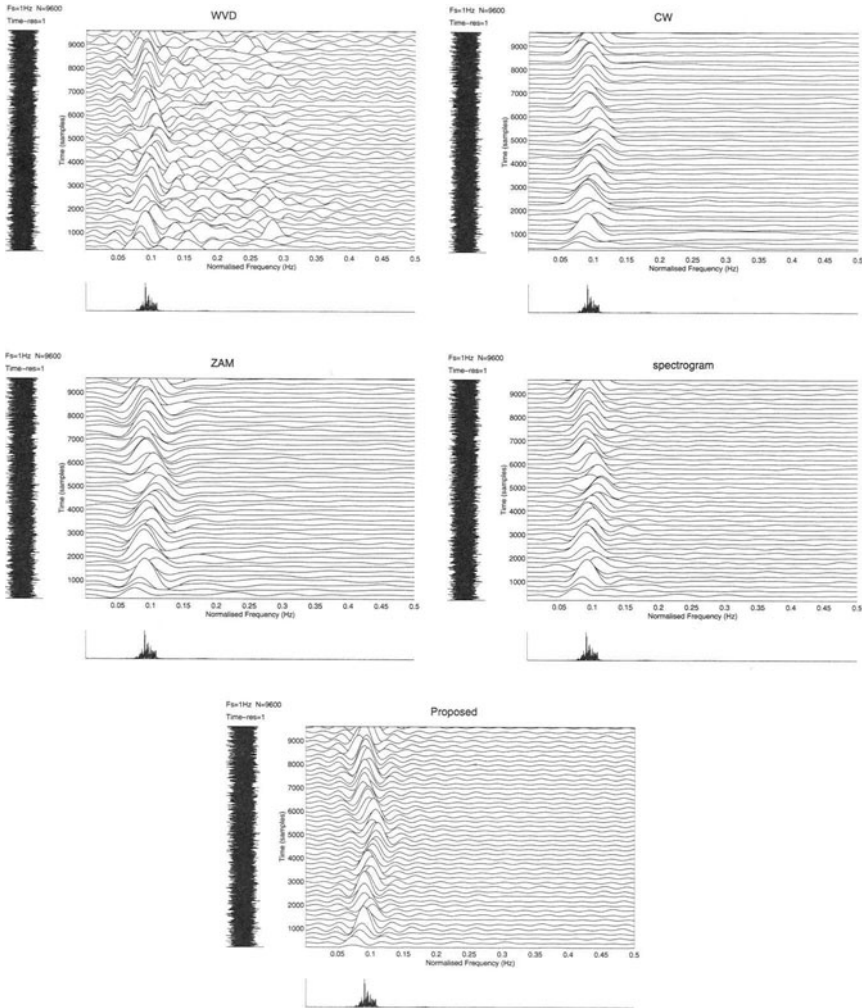


FIGURE 11.15. TFDs of a real-life multicomponent acoustic signal emitted from an overflying aircraft. The WVD (top left), the Choi–Williams distribution (top right), the Zhao–Atlas–Marks distribution (center left), the spectrogram (center right), and the B-distribution (bottom).

an IF estimator for linear FM signals. A statistical evaluation of the WVD-based IF estimator, for a linear FM signal in additive white Gaussian noise, has shown that this estimator is efficient [64], [68].

In practice, the implementation of the WVD necessitates a truncation of the signal in time, thus, the resulting WVD yields sinc functions around the signal IF. The sinc functions main lobes become narrower with increasing signal length.

This section shows that the WVD and the B-distribution are, in practice, equivalent for the analysis of a linear FM signal. Let us consider a linear FM signal whose

length is equal to $N = 129$ with a sampling frequency equal to unity. The signal is analyzed using both the WVD and the B-distribution with $\sigma = 1$. In Figure 11.16, we display slices of both distributions at the middle of the time interval. Note the equivalence, in terms of spectral resolution, of the two representations. This result suggests the use of the B-distribution as an IF estimator for a linear FM signal.

For statistical comparison between the two distributions, white Gaussian noise is added to the signal. The peak of the WVD and the peak of the B-distribution are used as IF estimators of the noisy linear FM signal at the middle of the time interval. We define the signal-to-noise ratio by $SNR = 10 \log_{10}(A^2/\sigma_w^2)$, where A is the signal amplitude taken equal to one and σ_w^2 is the noise variance. For each SNR value (varied by a 1 dB step), we run 1000 Monte Carlo simulations.

The simulations results are plotted in Figure 11.17. The “+” corresponds to the variance of the WVD-based IF estimator and the “o” corresponds to the variance of the B-distribution-based IF estimator. Note that for both distributions, the variances reach the Cramer–Rao bound (represented by the continuous line) and have almost the same threshold.

11.4.4 Discrete-time implementation of quadratic TFDs

11.4.4.1 Discrete-time TFDs and implementation aspects

In considering the general usefulness of TFDs, it is important to consider the properties of their discrete-time equivalents, and their ease of implementation.

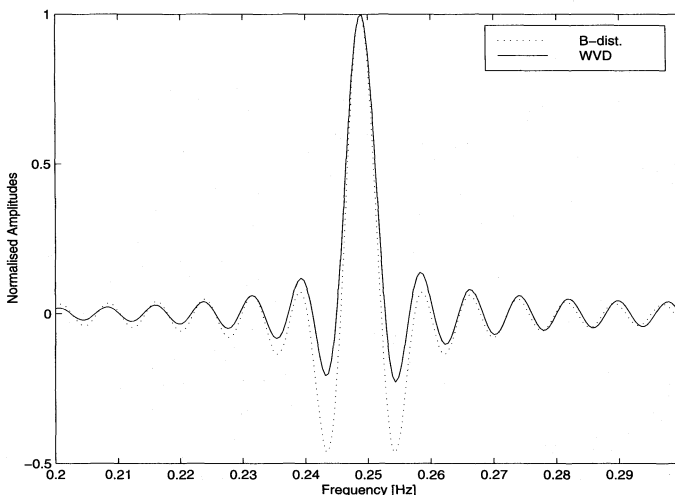


FIGURE 11.16. Slices of the WVD and the B-distribution ($\sigma = 1$) at the middle of the time interval for a linear FM signal. The signal length is equal to $N = 129$ and the sampling frequency is equal to unity.

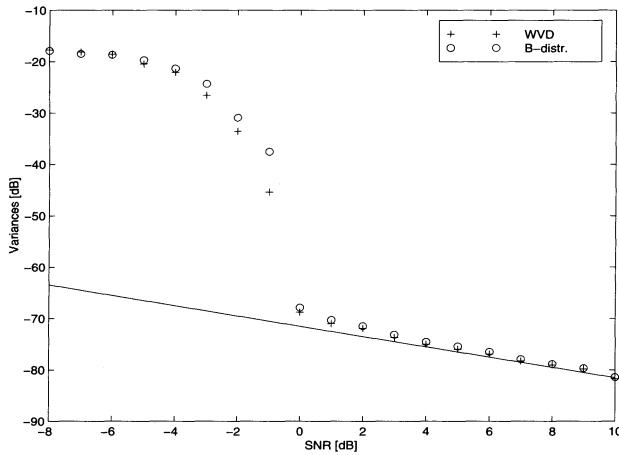


FIGURE 11.17. Variances of the WVD (“+”) and the B-distribution (“o”)-based IF estimator versus SNR for a linear FM signal in additive white Gaussian noise estimated at the middle of the time interval. The signal length is equal to $N = 129$ and the sampling frequency is equal to unity.

The discrete-time equivalent of the time-lag definition leads to a simple implementation of TFDs [1, p. 444]:

$$\rho_z(n, k) = \sum_{m \rightarrow k} \{G(n, m) * K_z(n, m)\}. \quad (11.4.28)$$

The implementation of these discrete-time quadratic TFDs requires three steps:

1. Formation of the quadratic kernel

$$K_z(n, m) = z(n + m) \cdot z^*(n - m).$$

2. Discrete convolution in time n with the smoothing function, $G(n, m)$.

3. Discrete FT with respect to m .

The implementation of Steps 1, 2, and 3 may be simplified by taking advantage of the many symmetries that exist, as explained in [35] and [69]. The WVD does not require Step 2 because its smoothing function, $G(n, m)$, equals $\delta(n)$.

Further details on the implementation and properties of TFDs are outlined in [2], Chapter 7, and [1, pp. 445–451]. Table 11.2 lists the discrete version of the time-lag kernel, $G(n, m)$, for some common TFDs. All these distributions have been implemented as part of a package which can be found on the web at: <http://www.sprc.qut.edu.au/tfsa>.

In the above expressions we assumed the signal to be analytic. Its calculation is shown in the next section.

TABLE 11.2. Discrete-time kernel function $G(n, m)$ for some quadratic TFDs. The discrete-time distribution, $\rho_z(n, k)$, is evaluated numerically using (11.4.28).

Time-frequency representation	Time-lag kernel $G(n, m)$
Windowed WVD	$\begin{cases} \delta(n) & m \in \left[\frac{-(M-1)}{2}, \frac{(M-1)}{2} \right], \\ 0 & \text{otherwise.} \end{cases}$
Pseudo-WVD using a rectangular window of odd length P	$\begin{cases} \frac{1}{P} & n \in \left[\frac{-(P-1)}{2}, \frac{(P-1)}{2} \right], \\ 0 & \text{otherwise.} \end{cases}$
Rihaczek–Margenau	$\frac{1}{2}[\delta(n+m) + \delta(n-m)].$
STFT using a rectangular window of odd length P .	$\begin{cases} \frac{1}{P} & m+n \leq \frac{(P-1)}{2}, \\ 0 & \text{otherwise.} \end{cases}$
Choi–Williams (parameter σ)	$\frac{\sqrt{\sigma/\pi}}{2m} e^{-\sigma n^2/4m^2}.$
B-distribution (parameter σ)	$\left[\frac{ m }{\cosh^2(n)} \right]^\sigma.$

11.4.4.2 Implementation of the analytic signal

There exist several techniques for the generation of the analytic signal. The most popular is the direct approach based on FT. The analytic signal, $z(n)$, corresponding to the real signal, $s(n)$, is obtained as follows:

1. Compute the N -point discrete Fourier transform (DFT) of $s(n)$ to obtain $S(k)$, $k = 0, 1, \dots, N - 1$.

2. Form the N -point one-sided transform as $Z(k) = \begin{cases} S(k), & k=0, \\ 2 \cdot S(k), & k=1, \dots, \frac{N}{2}-1, \\ 0, & \text{otherwise.} \end{cases}$

3. Calculate the analytic signal, $z(n)$, using $z(n) = \text{IDFT}[Z(k)]$, where IDFT is the inverse DFT.

An improved technique for the implementation of the analytic signal is proposed in [70].

11.5 Time-Frequency Analysis of Nonlinear FM Signals

11.5.1 Polynomial FM signals

Let us consider the problem of optimally representing and analyzing polynomial FM signals. The criterion of optimality considered here is to maximize the energy concentration, in the time-frequency domain, about the polynomial IF law of the signal.

Let the signal, $z(t)$, be of the form

$$z(t) = \text{rect}\left(\frac{t}{T}\right) A e^{j\phi(t)}, \quad (11.5.1)$$

where

$$\phi(t) = \sum_{i=0}^p a_i t^i. \quad (11.5.2)$$

The IF of the signal is defined as

$$f_i(t) = \frac{1}{2\pi} \frac{d\phi(t)}{dt}. \quad (11.5.3)$$

The case $p \leq 2$ corresponds to the class of signals for which the IF is either constant or linear. Such signals can be handled by the WVD [4].

The case $p > 2$, corresponds to the case of *nonlinear* polynomial FM signals, for which the WVD becomes inappropriate (see Section 11.5.2).

Nonlinear FM signals occur in both nature and man-made applications. For example, the sonar system of some bats often uses *hyperbolic* and *quadratic* FM signals for echo-location [71]. In radar, some of the pulse compression signals are *quadratic* FM signals [72]. In geophysics, in some modes of long-propagation of seismic signals, nonlinear signals may occur from earthquakes or underground nuclear tests [73]. In passive acoustics, the estimation of the altitude and speed of a propeller-driven aircraft is based on the instantaneous frequency which is a nonlinear function of time [74]. Nonlinear FM signals also appear in communications, astronomy, telemetry, and other engineering and scientific disciplines. It is therefore important to find appropriate analysis tools for such signals [75], [76], [77].

An approach that extends the conventional WVD to be able to analyze polynomial FM signals effectively is given in the forthcoming sections.

11.5.2 Optimality of the WVD for linear FM signals

The investigation of the notion of IF showed that the bilinearity of the WVD makes it optimal, in the sense of maximum energy concentration about the IF, for linear FM signals *only*. For nonlinear FM signals this optimal concentration is no longer assured and the WVD presents some artifacts. Moreover, the peak of the WVD, at any time instant t of the signal, is shifted from the real IF value. This

observation led to the design of *polynomial Wigner–Ville distributions* (PWVDs). These distributions are optimal for polynomial FM signals [78], [23], and they are able to solve problems that quadratic TFDs cannot [79], [80].

We describe in this section the key link between the WVD and the IF that makes it possible to design PWVDs which will exhibit a continuum of delta functions along the IF law for polynomial FM signals.

To explain how this is achieved, we describe the mechanism by which the WVD attains optimal concentration for a linear FM signal. Consider a unit amplitude analytic signal, $z(t) = e^{j\phi(t)}$. The WVD of this signal is defined by (11.3.26) and (11.3.27). Substitution of $z(t) = e^{j\phi(t)}$ in these equations yields

$$W_z(t, f) = \mathcal{F}_{\tau \rightarrow f} \left[e^{j(\phi(t+\tau/2) - \phi(t-\tau/2))} \right]. \quad (11.5.4)$$

Note that the term $\phi(t + \tau/2) - \phi(t - \tau/2)$ in (11.5.4) can be reexpressed as

$$\phi(t + \tau/2) - \phi(t - \tau/2) = 2\pi \hat{f}_i(t, \tau), \quad (11.5.5)$$

where $\hat{f}_i(t, \tau)$ can be considered to be an instantaneous frequency estimate. This estimate is the difference between two phase values divided by $2\pi\tau$, where τ is the separation in time of the phase values. This estimator is simply a scaled finite difference of phases centrally located about time instant t , and is known as the *central finite difference estimator* [81], [3]. The estimator follows directly from (11.5.3):

$$f_i(t) = \frac{1}{2\pi} \lim_{\tau \rightarrow 0} \left[\frac{\phi(t + \tau/2) - \phi(t - \tau/2)}{\tau} \right], \quad (11.5.6)$$

where τ has some finite nonzero value. Equation (11.5.4) can therefore be rewritten as

$$W_z(t, f) = \mathcal{F}_{\tau \rightarrow f} \left[e^{j2\pi\tau \hat{f}_i(t, \tau)} \right]. \quad (11.5.7)$$

Thus the WVD's quadratic kernel is seen to be a function which is reconstructed from the central finite difference derived IF estimate. This explains why the WVD yields good energy concentration for linear FM signals. Namely, the central finite difference estimator is known to be unbiased for such signals [3], and in the absence of noise, $\hat{f}_i(t, \tau) = f_i(t)$. Thus linear FM signals are transformed into sinusoids in the WVD kernel with the frequency of the sinusoid being equal to the instantaneous frequency of the signal, $z(t)$, at that value of time. Fourier transformation of the quadratic kernel then gives

$$W_z(t, f) = \delta(f - f_i(t)), \quad (11.5.8)$$

that is, a row of delta functions along the true IF of the signal. The above equation is valid only for linear FM signals. For nonlinear FM, we present a method referred to as the PWVD which extends the property of the WVD described by (11.5.8).

11.5.3 Design of polynomial Wigner–Ville distributions

The design of PWVDs which yield (11.5.8) for a nonlinear FM signal, is based on replacing the central finite difference estimator, which is inherent in the formulation of the WVD by an estimator which would be unbiased for polynomial FM signals. The general theory of polynomial phase difference coefficients estimation describes the procedure for deriving unbiased IF estimators for arbitrary polynomial FM signals [81], [82]. This procedure is briefly presented below in a discrete-time formulation.

11.5.3.1 Phase difference estimators for polynomial phase laws of arbitrary order

For the polynomial phase model given by (11.5.2), the instantaneous frequency is easily determined from (11.5.3) as

$$f_i(t) = \frac{1}{2\pi} \sum_{m=1}^p m a_m t^{m-1}. \quad (11.5.9)$$

For the discrete-time signal whose phase is defined by

$$\phi(n) = \sum_{m=0}^p a_m n^m, \quad (11.5.10)$$

the IF may be computed by the relation

$$f_i(n) = \frac{1}{2\pi} \phi(n) * d(n), \quad (11.5.11)$$

where $d(n)$ is an FIR differentiating filter [6], [81].

For phase laws which are linear or quadratic (i.e., for complex sinusoids or linear FM signals), the differentiating filter is a simple scaled phase differencer, known as the *central finite difference*. As the order of the phase polynomial increases, the filter then becomes a weighted sum of phase differences. The derivation in [6] determines the exact form of these higher-order phase difference based IF estimators [81].

The next section uses these generalized (or polynomial) phase difference IF estimators, to replace the central finite difference based IF estimator. The result of this replacement is a class of polynomial WVDs which ideally concentrate energy for polynomial phase signals along their instantaneous frequencies.

11.5.3.2 Noninteger powers form for PWVDs (form I)

The q th order unbiased IF estimator for polynomial phase signals can be expressed by [6]:

$$\hat{f}_i^{(q)}(t) = \frac{1}{2\pi\tau} \sum_{l=-q/2}^{q/2} b_l \phi \left(t + \frac{l\tau}{q} \right), \quad (11.5.12)$$

where q is an even integer number chosen such that $q \geq p$. The b_l coefficients are to be found so that in the absence of noise $\hat{f}_i^{(q)}(t) = f_i^{(q)}(t)$.

Now it is straightforward to define PWVDs with fractional powers of the signal as a generalization of (11.5.7):

$$W_z^{(q)}(t, f) = \mathcal{F}_{\tau \rightarrow f} \left\{ \exp\{j2\pi\tau \hat{f}_i^{(q)}(t, \tau)\} \right\} \quad (11.5.13)$$

$$= \mathcal{F}_{\tau \rightarrow f} \{K_z^{(q)}(t, \tau)\}, \quad (11.5.14)$$

where $\hat{f}_i^{(q)}(t, \tau)$ is the estimator given by (11.5.12), centrally located about time instant, t .

For a unit amplitude signal, $A = 1$ in (11.5.1), it follows from (11.5.12), (11.5.13), and (11.5.14) that

$$K_z^{(q)}(t, \tau) = \exp \left\{ j \sum_{l=-q/2}^{q/2} b_l \phi \left(t + \frac{l\tau}{q} \right) \right\} \quad (11.5.15)$$

$$= \prod_{l=-q/2}^{q/2} \left[z \left(t + \frac{l\tau}{q} \right) \right]^{b_l}. \quad (11.5.16)$$

We refer to this form of PWVDs as the “fractional powers form” since the coefficients b_l are, in general, rational numbers.

Note also that $K_z^{(q)}(t, \tau)$ is a *multilinear kernel*. While the WVD’s (quadratic) kernel transforms linear FM signals into sinusoids, the PWVD (multilinear) kernel is designed to transform higher-order FM signals into sinusoids. These sinusoids manifest as delta functions when Fourier transformed. Thus the WVD may be interpreted as a method based on just the first-order approximation in a polynomial expansion of phase differences.

A detailed procedure for the evaluation of the b_l coefficients is given in [6]. Another method that leads to the same results was recently proposed by Benidir in [82].

Since the expected value of the “fractional powers” form of the PWVD cannot be interpreted as conventional time-varying polyspectra, we present an alternative form of the PWVD, where the signal, $z(n)$, is raised to integer powers.

11.5.3.3 Integer powers form for PWVDs (form II)

An alternative way of implementing unbiased IF estimators for arbitrary polynomial phase laws requires that we weight the phases at unequally spaced samples and then take their sum. This allows the weights, (b_l) , to be prespecified to integer values. The IF estimator of this type is defined as [78]:

$$\hat{f}_i^{(q)}(t, \tau) = \frac{1}{2\pi\tau} \sum_{l=-q/2}^{q/2} b_l \phi(t + c_l \tau). \quad (11.5.17)$$

Here c_l are coefficients which control the separation of the different phase values used to construct the IF estimator. Coefficients b_l and c_l may be varied to yield

unbiased IF estimates for signals with an arbitrary polynomial FM law. The procedure for determining the b_l and c_l coefficients for the case $q = 4$ is illustrated in the next section. While the b_l may theoretically take any values, they are practically constrained to be integers, since the use of integer b_l enables the expected values of the PWVD to be interpreted as time-varying higher-order spectra. This important fact will make the form II of the PWVD preferable, and further on in the text, form II will be assumed, unless otherwise stated.

The PWVDs which result from incorporating the estimator in (11.5.17) are defined analogously to (11.5.13) and (11.5.14), again assuming constant amplitude, A . The multilinear kernel of the PWVD is given by

$$K_z^{(q)}(t, \tau) = \prod_{l=-q/2}^{q/2} [z(t + c_l \tau)]^{b_l}. \quad (11.5.18)$$

The above expression for the kernel may be rewritten in a symmetric-type form according to

$$K_z^{(q)}(t, \tau) = \prod_{l=0}^{q/2} [z(t + c_l \tau)]^{b_l} [z^*(t + c_{-l} \tau)]^{-b_{-l}}. \quad (11.5.19)$$

The discrete-time version of the PWVD is given by the discrete FT of

$$K_z^{(q)}(n, m) = \prod_{l=0}^{q/2} [z(n + c_l m)]^{b_l} [z^*(n + c_{-l} m)]^{-b_{-l}}, \quad (11.5.20)$$

where $n = tf_s$, $m = \tau f_s$, and f_s is the sampling frequency.

The WVD is a special case of the PWVD and may be recovered by setting $q = 2$, $b_{-1} = -1$, $b_0 = 0$, $b_1 = 1$, $c_{-1} = -\frac{1}{2}$, $c_0 = 0$, $c_1 = \frac{1}{2}$. A list of properties for the PWVD is given in [5].

11.5.3.4 Design of the PWVD (form II) for quadratic and cubic FM signals

Since $p = 3$ for quadratic FM, or $p = 4$ for cubic FM, we set $q = 4$ to account for both cases. The set of coefficients b_l and c_l must be found to completely specify the new kernel. The coefficients must then be found such that the PWVD kernel transforms unit amplitude cubic, quadratic, or linear FM signals into sine waves. The design procedure necessitates setting up a system of equations which relate the polynomial IF of the signal to the IF estimates obtained from the polynomial phase differences, and solving for the c_l . In setting up the design equations it is assumed that the signal phase in discrete-time form is a p th-order polynomial, given by

$$\phi(n) = \sum_{i=0}^p a_i n^i, \quad (11.5.21)$$

where the a_i are the polynomial coefficients. The corresponding IF is then given by

$$f_i(n) = \frac{1}{2\pi} \sum_{i=1}^p ia_i n^{i-1}. \quad (11.5.22)$$

A q th order phase difference estimator ($q \geq p$) is applied to the signal and it is required that, at any discrete-time index, n , the output of this estimator gives the true IF. The required system of equations to ensure this is

$$\frac{1}{2\pi m} \sum_{l=-q/2}^{q/2} b_l \phi(n + c_l m) = f_i(n), \quad (11.5.23)$$

that is,

$$\frac{1}{2\pi m} \sum_{l=-q/2}^{q/2} b_l \sum_{i=0}^p a_i (n + c_l m)^i = \frac{1}{2\pi} \sum_{i=1}^p ia_i n^{i-1}. \quad (11.5.24)$$

The resulting discrete-time kernel is then given by

$$K_z^{(4)}(n, m) = [z(n + 0.675m)z^*(n - 0.675m)]^2 z^*(n + 0.85m)z(n - 0.85m). \quad (11.5.25)$$

Note. The solution given above is just one of an infinite number of possible solutions. For more details on the design procedure, the reader is referred to [23], [83], and [84].

Figure 11.18 illustrates the conventional WVD, the PWVD _{$q=4$} [5], and the PWVD _{$q=6$} [5] of the same quadratic FM signal (noiseless case), respectively. The superior behavior of the latter is indicated by the sharpness of the peaks in Figure 11.18(b) and (c). From the peaks of the PWVD the quadratic IF law can be recovered easily. The conventional WVD, on the other hand, shows many oscillations that tend to degrade its performance.

Implementation Issue. Several important points were made concerning the practical implementation of the kernel in (11.5.25). These were reported in [85] and [6].

11.5.3.5 The Wigner–Ville trispectrum

In the same way as the WVD can be interpreted as the core of the class of quadratic TFDs, the PWVD can be used to define a class of multilinear or higher-order TFDs [78]. Alternative forms of higher-order TFDs, as extensions of the quadratic class of TFDs, were proposed by several authors [86], [87], [88], [89]. Note that the general class of higher-order TFDs can be defined in the multitime–multifrequency space, as a method for time-varying higher-order spectral analysis. However, in this approach, we choose to project the full multidimensional space onto the time-frequency subspace, in order to obtain specific properties (such as time-frequency representation of polynomial FM signals) [90].

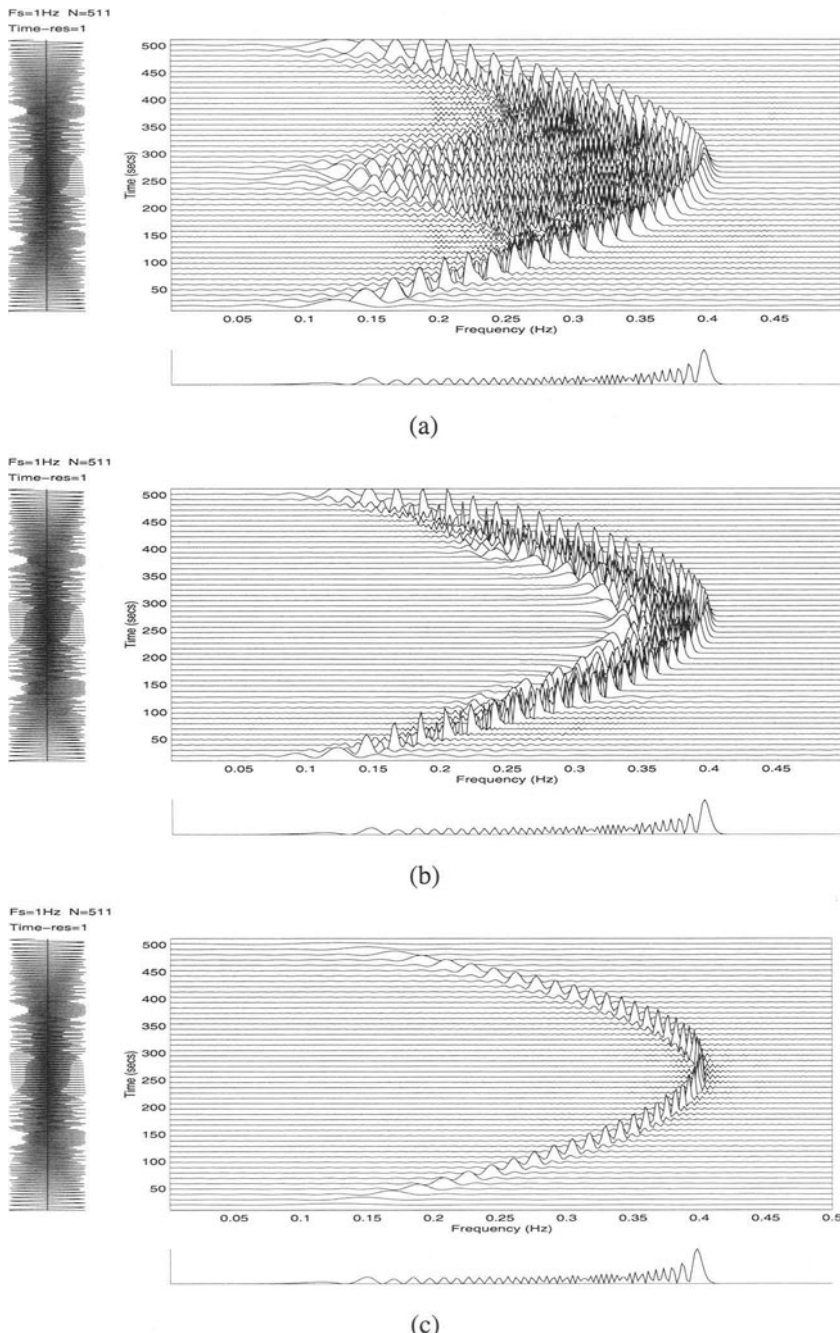


FIGURE 11.18. Time-frequency representations of a quadratic FM signal: (a) WVD; (b) $\text{PWVD}_{q=4}$; and (c) $\text{PWVD}_{q=6}$.

The Wigner–Ville trispectrum (WVT) of a random signal, $z(t)$, is defined as [5]:

$$\mathcal{W}_z^{(4)}(t, f) = \text{E} \left\{ \int_{-\infty}^{\infty} z^2 \left(t + \frac{\tau}{4} \right) \left[z^* \left(t - \frac{\tau}{4} \right) \right]^2 e^{-j2\pi f \tau} d\tau \right\}, \quad (11.5.26)$$

where $\text{E}\{\cdot\}$ is the expected value.

The WVT is actually a reduced form of the full WVT that was defined in [86] and [88] as follows:

$$\begin{aligned} \mathcal{W}_z^{(4)}(t, f_1, f_2, f_3) &= \text{E} \int_{\tau_1} \int_{\tau_2} \int_{\tau_3} z^* \left(t - \frac{\tau_1 + \tau_2 + \tau_3}{4} \right) \cdot z \left(t + \frac{3\tau_1 - \tau_2 - \tau_3}{4} \right) \\ &\quad \times z \left(t + \frac{3\tau_2 - \tau_1 - \tau_3}{4} \right) \cdot z^* \left(t + \frac{3\tau_3 - \tau_1 - \tau_2}{4} \right) \prod_{i=1}^3 e^{-j2\pi f_i \tau_i} d\tau_i \end{aligned} \quad (11.5.27)$$

and is obtained from (11.5.27) by selecting $\tau_1 = \tau_2 = \tau/2$, $\tau_3 = 0$, and $f_1 = f_2 = f_3 = f$. For simplification, we use the term WVT to refer to the reduced form.

Cumulant-Based Fourth Order Spectra. There are a number of ways of forming a cumulant-based WVT [87], [90]. In [90], the authors proposed

$$\begin{aligned} \mathcal{C}_z^{(4)}(t, \tau) &= \text{E} \left\{ z^2 \left(t + \frac{\tau}{4} \right) \left[z^* \left(t - \frac{\tau}{4} \right) \right]^2 \right\} - 2 \left[\text{E} \left\{ z \left(t + \frac{\tau}{4} \right) z^* \left(t - \frac{\tau}{4} \right) \right\} \right]^2 \\ &\quad - \text{E}\{z^2(t)\} \cdot \text{E}\{z^*(t)^2\}. \end{aligned} \quad (11.5.28)$$

This definition has the advantage that it is a natural extension of Dwyer's fourth-order spectrum [91], and hence can detect Gaussian amplitude modulated linear FM signals [83].

11.5.4 Multicomponent signals and polynomial TFDs

Until now we have considered the PWVD of only single-component FM signals. That is, signals limited to only one time-varying feature in the frequency domain. In both natural and man-made signals, it is much more common to encounter *multicomponent* signals. It is therefore important to see if and how polynomial TFDs can be used for multicomponent signal analysis.

11.5.4.1 Cross-terms in the PWVD

Since the PWVDs and their respective polynomial TFDs are multilinear representations, they suffer from the presence of cross-terms. For example, let us consider a deterministic complex signal

$$z(t) = e^{j2\pi(f_1 t + \alpha_1 t^2)} + e^{j2\pi(f_2 t + \alpha_2 t^2)} \quad (11.5.29)$$

and let us derive expressions for the WVT defined in (11.5.27) in this case.

The kernel of the WVT ($\tau_1 = \tau_2 = \tau/2$) is

$$\begin{aligned} K_z^{(4)}(t, \tau) &= [z(t + \tau/4)]^2 [z^*(t - \tau/4)]^2 \\ &= e^{j2\pi f_1 \tau} + e^{j2\pi f_2 \tau} + 4e^{j2\pi[(f_1 + f_2)/2]\tau} \\ &\quad + 4 \cos 2\pi(f_1 - f_2)t [e^{j2\pi[(3f_1 + f_2)/4]\tau} + e^{j2\pi[(f_1 + 3f_2)/4]\tau}] \\ &\quad + 2 \cos 4\pi(f_1 - f_2)t e^{j2\pi[(f_1 + f_2)/2]\tau}. \end{aligned} \quad (11.5.30)$$

The first two terms in (11.5.30) represent the auto-terms. The last two terms are the cross-terms with time-oscillating amplitudes. It is the cross-term, $4 \exp\{j2\pi[(f_1 + f_2)/2]\tau\}$, which causes a serious problem, since it has a constant amplitude, just as if it was a self-term. This cross-term is indistinguishable from self-terms without some a priori knowledge. Integration of the WVT over time yields

$$\int W_z^{(4)}(t, f) dt = \delta(f - f_1) + \delta(f - f_2) + 4\delta\left(f - \frac{f_1 + f_2}{2}\right). \quad (11.5.31)$$

The spike at $(f_1 + f_2)/2$ frequency is due to this nonoscillating cross-term. The implication of this simple analysis is that PWVDs exhibit some cross-terms which cannot be handled by standard smoothing functions (such as the reduced interference method [56] or cone-shaped method [57]).

To proceed further, we consider the general multilinear TFD whose projection to the time-frequency domain yields the WVT, i.e., we abandon slicing in the multilag domain and consider the WVT in a full multifrequency domain, as given by (11.5.27). As an intermediate step, consider the kernel function in (t, τ_1, τ_2) (where τ_1 and τ_2 are now two independent variables) applied to the same signal

$$K_z^{(4)}(t, \tau_1, \tau_2) = [z(t + \tau_1/2)]^2 [z^*(t - \tau_2/2)]^2. \quad (11.5.32)$$

Then

$$\int W_z^{(4)}(t, \nu_1, \nu_2) dt = \int \tau_1 \xrightarrow{\mathcal{F}} \nu_1 \quad \tau_2 \xrightarrow{\mathcal{F}} \nu_2 \{K_z^{(4)}(t, \tau_1, \tau_2)\} dt \quad (11.5.33)$$

$$\begin{aligned} &= \delta(\nu_1 - f_1)\delta(\nu_2 - f_1) \\ &\quad + \delta(\nu_1 - f_1)\delta(\nu_2 - f_2) \\ &\quad + 2\delta\left(\nu_1 - \frac{f_1 + f_2}{2}\right)\delta\left(\nu_2 - \frac{f_1 + f_2}{2}\right) \\ &\quad + \delta(\nu_1 - f_2)\delta(\nu_2 - f_1) \\ &\quad + \delta(\nu_1 - f_2)\delta(\nu_2 - f_2). \end{aligned} \quad (11.5.34)$$

Thus, by taking a diagonal slice in the (τ_1, τ_2) plane, i.e., $\tau_1 = \tau_2 = \tau/2$ (which corresponds to the WVT), we effectively project the bifrequency (ν_1, ν_2) domain to its slice, $\nu_1 = \nu_2 = \nu$. Thus, (11.5.31) is a projection of the bifrequency domain (ν_1, ν_2) onto $\nu_1 = \nu_2 = \nu$. Similarly, by taking a slice $\tau_1 = 0; \tau_2 = \tau$, we effectively project the bifrequency (ν_1, ν_2) to its slice $\nu_1 = 0, \nu_2 = \nu$.

If we go a step further and evaluate the WVT as given by (11.5.27), of the same signal, $z(t)$, we obtain

$$\begin{aligned} \int W_z^{(4)}(t, \nu_1, \nu_2, \nu_3) dt &= \delta(\nu_1 - f_1)\delta(\nu_2 - f_1)\delta(-\nu_3 - f_1) \\ &\quad + \delta(\nu_1 - f_2)\delta(\nu_2 - f_2)\delta(-\nu_3 - f_2) \\ &\quad + \delta(\nu_1 - f_2)\delta(\nu_2 - f_1)[\delta(\nu_3 + f_1) + \delta(\nu_3 + f_2)] \\ &\quad + \delta(\nu_1 - f_1)\delta(\nu_2 - f_2)[\delta(\nu_3 + f_1) + \delta(\nu_3 + f_2)] \end{aligned} \quad (11.5.35)$$

or, for the slice at $\nu_1 = \nu_2 = -\nu_3 = \nu$:

$$\int W_z^{(4)}(t, \nu) dt = \delta(\nu - f_1) + \delta(\nu - f_2). \quad (11.5.36)$$

Hence, by taking a proper slice in a multifrequency (rather than multilag) domain one can avoid nonoscillating cross-terms of the WVT. The same conclusion applies to the PWVD _{$q=4$} .

Consider now a two-impulse signal: $z(t) = \delta(t - t_1) + \delta(t - t_2)$. The slice of $W_z^{(4)}(t, \nu_1, \nu_2, \nu_3, \nu_4)$ along $\nu_1 = \nu_2 = -\nu_3 = \nu$ projected to the frequency axis yields

$$\int W_z^{(4)}(t, \nu) d\nu = \delta(t - t_1) + \delta(t - t_2) + 4\delta\left(t - \frac{t_1 + t_2}{2}\right) \quad (11.5.37)$$

which indicates the presence of a nonoscillating cross-term with four times greater amplitude than the auto-terms.

On the basis of this analysis, we can observe that there is no simple solution for multicomponent FM signals using higher-order WVDs, because that solution would require the following two contradicting demands to be fulfilled: in order to avoid nonoscillating cross-terms we are forced to take slices in the multifrequency domain (as demonstrated by (11.5.35) and (11.5.36)); in order to eliminate self artifacts of monocomponent nonlinear FM signals, we must take proper slices in the multilag domain (the PWVD _{$q=4$} is such an example). Since both conditions cannot be satisfied simultaneously, we can develop only suboptimal solutions, some of which are described in [80], [22], and the next section.

11.5.4.2 Cross-terms suppression in the PWVD

The filtering of cross-terms of the quadratic (or second-order) TFDs is best performed in the *ambiguity domain*. This approach is extended to the filtering of cross-terms of time-varying higher-order moments, specifically those used to form polynomial TFDs. The methodology involves first determining the two-dimensional inverse FT of the polynomial TFD; this is the *polynomial ambiguity function*. This function is then multiplied by a two-dimensional low-pass filtering function, which should reduce the cross-term level. A further two-dimensional Fourier inversion then recovers the smoothed polynomial TFD.

One smoothed polynomial TFD which is of particular interest is the one obtained with the reduced interference smoothing function [6]. It is also possible to smooth

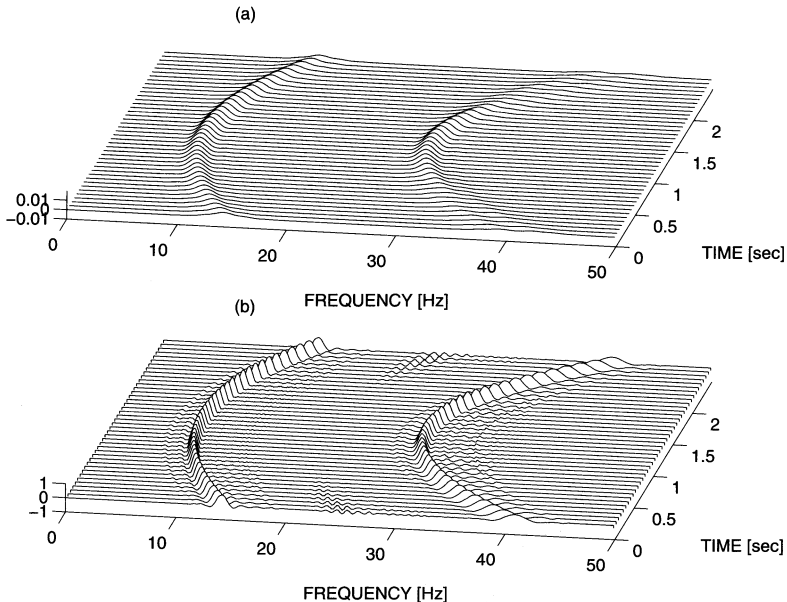


FIGURE 11.19. (a) The spectrogram, and (b) the sixth-order polynomial TFD implemented using the S-method of the same signal consisting of two quadratic FM components.

multidimensional higher order moment functions (as opposed to “reduced” two-dimensional moment functions) in the ambiguity domain. In this case, however, it is necessary to define higher-order ambiguity functions [6].

In a related method originally proposed for the detection of chirps, [92], different instantaneous moment function slices are summed up in the ambiguity domain in order to reduce the cross-terms. The reasoning behind this method is based on the fact that auto-terms of different slices always appear at the same position, and hence they add up. On the contrary, the position of cross-terms depends on the particular slice, and in summation they tend to cancel out.

Lately, the recursive S-method was introduced [93]. It was shown that, by a suitable selection of a window length, it is possible to reduce the cross-terms while having highly concentrated TFD around the IF. Recently, the S-method was applied to the PWVD [94]. The proposed PWVD implementation was shown to yield the sum of the PWVD of each component separately, thereby removing the cross-terms [83] (see Figure 11.19).

11.5.4.3 Multicomponent separation using time-varying higher-order spectra

Time-varying higher-order spectra can be calculated from these multidimensional higher-order ambiguity functions in much the same way as they are calculated for the second-order case. That is, if an ensemble of signals is available, then the higher-order spectra may be obtained by ensemble averaging the higher-order ambiguity functions, followed by multidimensional Fourier inversion. If, however,

there is not an ensemble, one has to estimate the expected value of the higher-order ambiguity function by time and multilag averaging.

It has also been recently shown in [83] and [22] that the cumulant WVT (C-WVT) preserves the essential properties of cumulant HOS (i.e., suppression of Gaussian additive noise, superposition of independent multicomponent random signals) and characterizes the time-varying frequency content of non-Gaussian random signals (see Figures 11.20(a) and (b)).

These properties of the C-WVT were verified for FM signals affected by multiplicative and additive noise in [83]. An application of the WVT in mobile communications affected by Rayleigh fading has recently been reported in [95].

11.5.5 IF estimation using the PWVD

In many real-life applications such as radar, sonar, biomedical engineering, and automotive signals, the IF characterizes important physical parameters of the signals [67], [19]. Therefore, it is desirable to have fast and effective methods for direct IF estimation. The problem of IF estimation was comprehensively treated in [3] and [4]. This section presents some recent developments that relate to nonlinear FM signals.

Two major approaches exist in the literature for IF estimation. One approach assumes a certain form of the signal and uses a mathematical model to estimate it. This is referred to as a parametric approach. Some problems limit its application in that it is difficult to find the “correct” mathematical model of the signal. Furthermore, signal parameters estimation becomes cumbersome as the order of nonlinearity of the signal increases. Alternatively, one may use a nonparametric approach for IF estimation. A well-known class of nonparametric methods is based on TFDs. The time-frequency analysis ability to display and characterize the time-varying spectral contents of nonstationary signals made it a natural technique for IF localization and estimation.

The PWVD gives maximum energy concentration along the IF law for polynomial FM signals. For this reason, its peak was proposed as an IF estimator for polynomial FM signals embedded in white Gaussian noise [23]. A full and detailed statistical performance evaluation of this estimator can be found in [68] where the estimator was shown to be unbiased.

In [96], Barkat et al. considered a more general situation; that is, using the PWVD peak to estimate the IF of an *arbitrary nonlinear*, not necessarily polynomial, FM signal embedded in white Gaussian noise. In this case, there is a systematic error or “bias” in the estimator due to the mismatch of the signal with the distribution order. Moreover, they considered the analysis window to be time-varying and of arbitrary shape. The authors derived analytical expressions for the bias as well as the asymptotic variance of the IF estimator and showed that these quantities are highly signal-dependent and tend to vary inversely as a function of the analysis window length. Based on this observation, they derived an expression for the optimal window length that minimizes the mean square error for the IF estimator and proposed an algorithm to design the “best” or optimal PWVD in the sense of

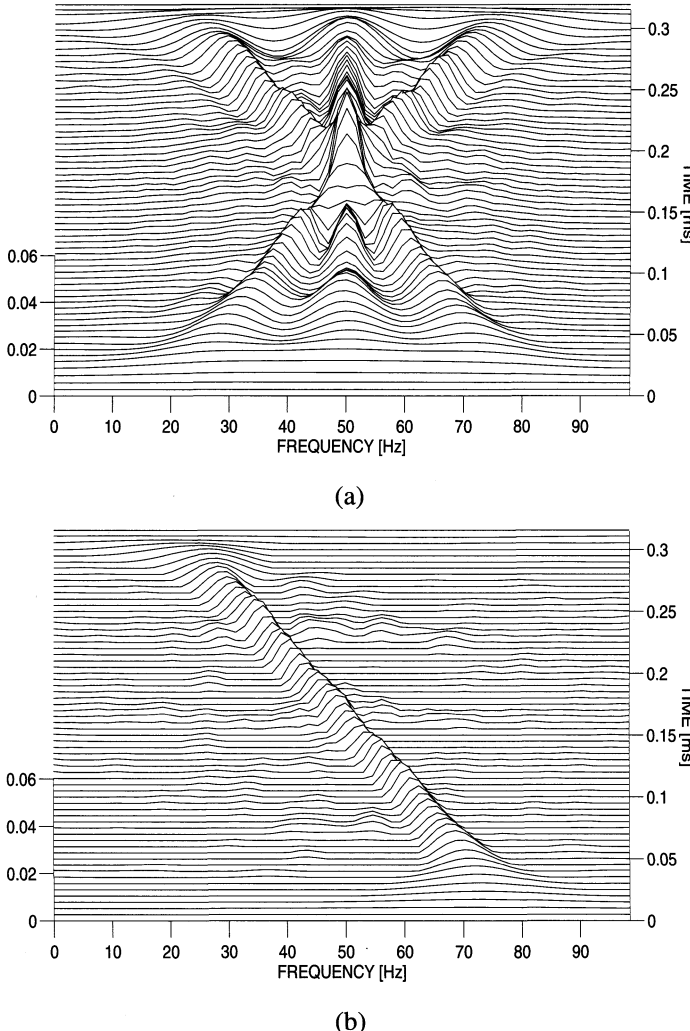


FIGURE 11.20. A composite signal consisting of a Gaussian and a non-Gaussian component: (a) estimate of the M-WVT (notice the cross-terms in the bispectrum plane); (b) estimate of the C-WVT.

resolving the bias-variance tradeoff. The work presented in [96] is an extension of the works in [97], [98] where the windowing in the WVD and the spectrogram were considered.

As an illustration, let us consider the IF estimation of a highly nonlinear FM signal. Since, in this case, the IF is better approximated by a high degree polynomial, it is preferred to use the PWVD of order 6 rather than the WVD (which is a PWVD of order 2) in the estimation (the WVD would have a larger bias). First, the PWVD with a fixed but small window length is used. Then, the PWVD with a fixed but

large window length is used. In the third case, the adaptive optimal window length in the PWVD is used. Simulation results, presented in Figure 11.21, show that the proposed algorithm can estimate the signal IF more accurately than the other two constant window time-frequency based estimators.

The same experiment was performed using a different signal whose IF is also highly nonlinear. Figure 11.22 displays the obtained results. Again, the same conclusion as that of the first experiment can be made. In fact, the proposed algorithm was found to outperform any IF estimator based on a constant window time-frequency distribution.

The algorithm was compared with other existing IF estimation techniques such as the LMS, RMS, and CFD [81]. Figure 11.23 displays the IF estimates of the signal of the second experiment above when the LMS, RLS, and CFD are used in the estimation. Note the superiority of the adaptive window PWVD algorithm (Figure 11.22(c)) compared to these techniques (Figure 11.23).

Acknowledgments: The authors would like to acknowledge the Australian Research Committee for funding some of the work reported in this chapter. This chapter is largely based on a tutorial given by the first author at the ISPACS workshop held in Melbourne in October 1998.

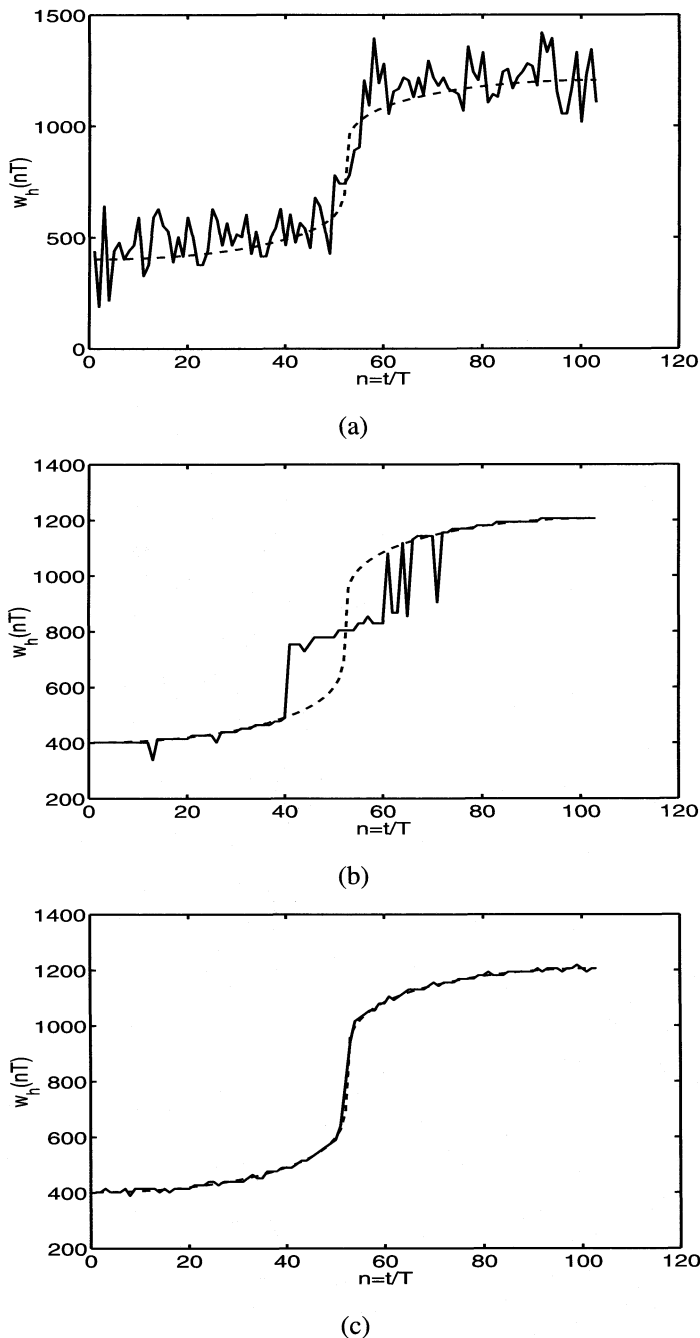


FIGURE 11.21. The IF estimates of a highly nonlinear FM signal using a windowed PWVD of order 6. In (a) a small window is used, in (b) a large window is used, and in (c) an adaptive window is used.

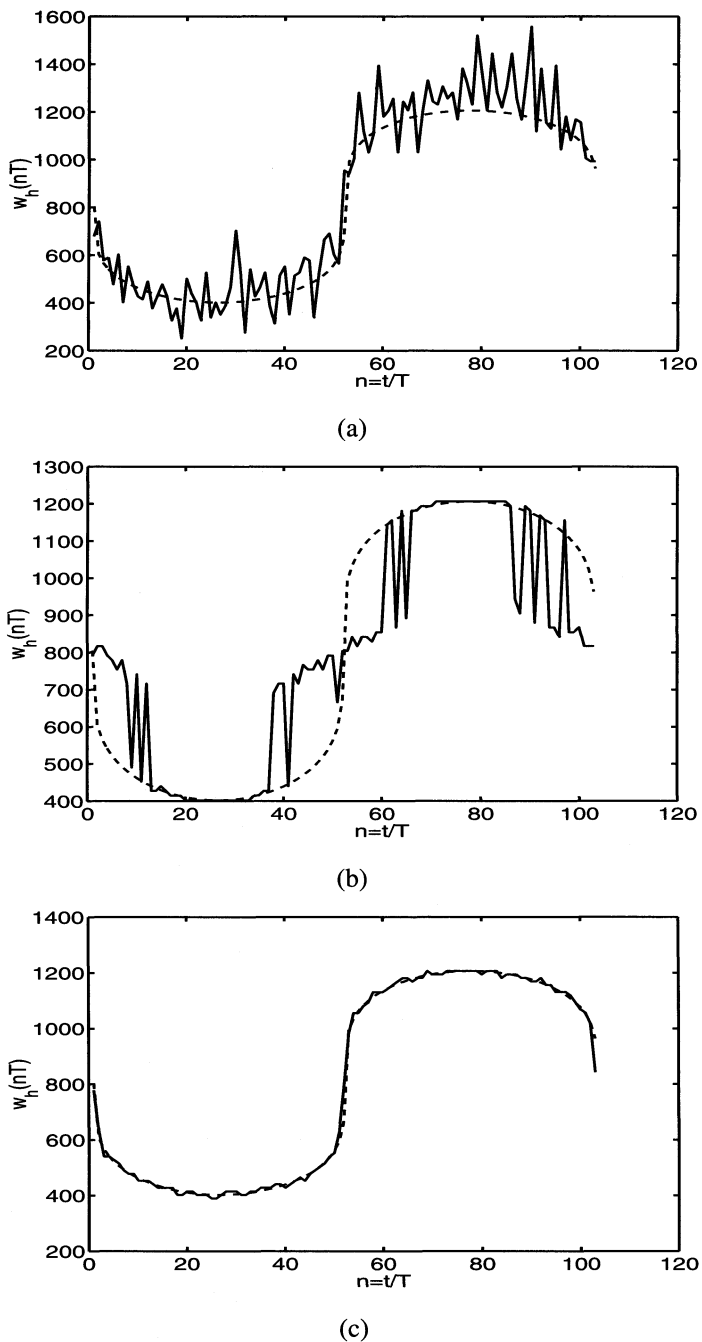


FIGURE 11.22. The IF estimates of another highly nonlinear FM signal using a windowed PWVD of order 6. In (a) a small window is used, in (b) a large window is used, and in (c) an adaptive window is used.

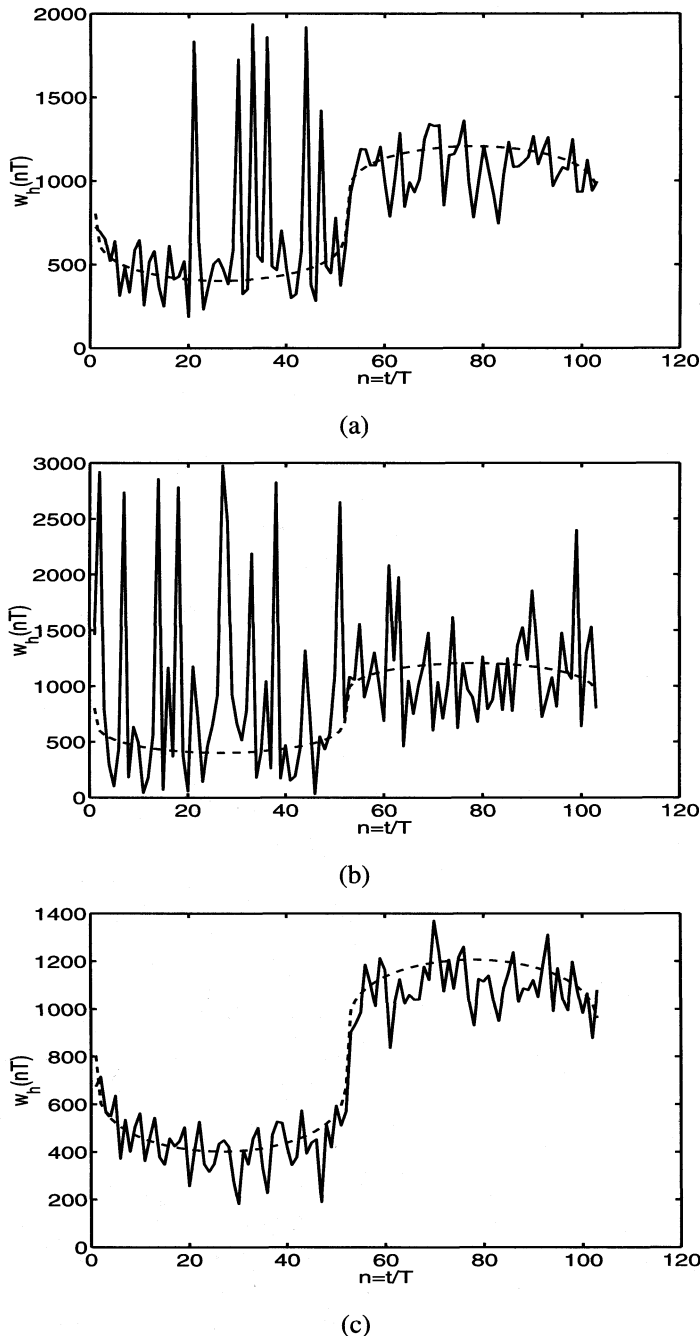


FIGURE 11.23. The IF estimates of the same signal as in Figure 11.22 using (a) the CFD estimator, (b) the LMS estimator, and (c) the RLS estimator.

References

- [1] B. Boashash. Time-frequency signal analysis, in *Advances in Spectrum Analysis and Array Processing*, (S. Haykin, ed.), Vol. 1, Chap. 9, pp. 418–517, Prentice-Hall, Englewood Cliffs, NJ, 1991.
- [2] B. Boashash, ed. *Time Frequency Signal Analysis*, Longman Cheshire, Melbourne, 1992.
- [3] B. Boashash. Interpreting and estimating the instantaneous frequency of a signal. Part I: Fundamentals. *Proceedings of the IEEE*, pp. 520–538, April, 1992.
- [4] B. Boashash. Interpreting and estimating the instantaneous frequency of a signal. Part II: Algorithms. *Proceedings of the IEEE*, 539–569, April, 1992.
- [5] B. Boashash and B. Ristic. A time-frequency perspective of higher-order spectra as a tool for non-stationary signal analysis, In *Higher-Order Statistical Signal Processing*, (B. Boashash and E. J. Powers and A. M. Zoubir, eds.), Chap. 4, Longman Cheshire, London, 1995.
- [6] B. Boashash, Time-frequency signal analysis, past, present and future trends, in *Control and Dynamic Systems*, (C. T. Leonides, ed.), Vol. 78—*Digital Control and Signal Processing Systems and Techniques*, Chap. 1, pp. 1–71, Academic Press, New York, 1996.
- [7] B. Boashash. An introduction to time-frequency signal analysis, in *Proceedings of the Sixth IEEE Inter. Workshop on Intell. Sig. Proc. and Com. Systems*, Melbourne, 4–6 Nov. 1998 (Tutorial)
- [8] D. Gabor. Theory of Communication, *J. of IEE*, **93** (1946), 429–457.
- [9] J. Ville. Theorie et application de la notion de signal analytique, *Cables et Transmissions* **2A** (1) (1948) 61–74.
- [10] C. H. Page. Instantaneous power spectra, *J. of Appl. Phys.* **23**(1) (1953), 103–106.
- [11] C. Turner. On the concept of an instantaneous power spectra and its relation to the autocorrelation function, *J. of Appl. Phys.* **25** (1954), 1347–1351.
- [12] M. Levin. Instantaneous spectra and ambiguity function, *IEEE Trans. Inform. Theory*, **13** (1967), 95–97.
- [13] A. Rihaczek. Signal energy distribution in time and frequency, *IEEE Trans. Inform. Theory* **14**(3) (1968), 369–374.
- [14] B. Boashash, B. Escudie and J. Komatitsch. Sur la possibilité d'utiliser la représentation conjointe en temps et fréquence dans l'analyse des signaux modulés en fréquence émis en vibroismiques, in *7th Symposium on Signal Processing and its Applications*, pp. 121–126, 1979.
- [15] T. A. C. M. Classen and W. F. G. Mecklenbrauker. The Wigner distribution—Part 1, *Phillips J. Res.* **35** (1980), 217–250.
- [16] T. A. C. M. Classen and W. F. G. Mecklenbrauker. The Wigner distribution—Part 2, *Phillips J. Res.* **35** (1980), 276–300.

- [17] T. A. C. M. Classen and W. F. G. Mecklenbrauker. The Wigner distribution—Part 3, *Phillips J. Res.* **35** (1980), 372–389.
- [18] B. Boashash, P. Flandrin, B. Escudie, and J. Grea. Positivity of time-frequency distributions, *C. R. Acad. Sci. Paris*, (1979).
- [19] B. Boashash. Wigner analysis of time-varying signals—Its application in seismic prospecting, in *Proc. EUSIPCO*, pp. 703–706, 1983.
- [20] B. Boashash. Representation conjointe en temps et en fréquence des signaux d'énergie finie, Technical Report 373 78, Elf-Aquitaine Research Publication, 1978.
- [21] J. Jeong and W. J. Williams, Kernel design for reduced interference distributions, *IEEE Trans. Signal Process.* **40**(2) (1992), 402–412.
- [22] B. Ristic. Signal dependent and higher-order time-frequency analysis, PhD thesis, Signal Processing Research Centre, Queensland University of Technology, Australia, 1995.
- [23] B. Boashash and P. J. O'Shea. Polynomial Wigner–Ville distributions and their relationship to time-varying higher-order spectra, *IEEE Trans. Signal Process.* **42** (1994), 216–220.
- [24] G. Jones. Time-frequency analysis and the analysis of multicomponent signals, PhD thesis, Queensland University of Technology, 1992.
- [25] J. Kay and R. Lerner. *Lectures in Communications Theory*, McGraw-Hill, New York, 1961.
- [26] C. Helstrom. An expansion of a signal into Gaussian elementary signals, *IEEE Trans. Inform. Theory* **13** (1966), 344–345.
- [27] I. Daubeshies. The wavelet transform: A method for time-frequency localisation, in *Advances in Spectral Estimation and Array Processing*, (S. Haykin, ed.), Prentice Hall, Englewood Cliffs, NJ, 1990.
- [28] L. Cohen. Time-frequency distributions—A review, *Proc. IEEE*, **77** (1989), 941–981.
- [29] B. Boashash. Note on the use of the Wigner distribution, *IEEE Trans. Acoustics, Speech Signal Process.* **36**(9) (1988), 1518–1521.
- [30] E. P. Wigner. On the quantum correction for thermodynamic equilibrium, *Phys. Rev.* **40** (1932), 748–759.
- [31] B. Boashash. Representation temps-fréquence. PhD thesis, Dipl. de Docteur Ingénieur these, University of Grenoble, 1982.
- [32] B. Boashash. Note d'information sur la représentation des signaux dans le domaine temps-fréquence, Technical Report, 135 81, Elf-Aquitaine Research Publication, 1981.
- [33] W. Martin. Time-frequency analysis of random signals, in *ICASSP*, pp. 1325–1328, 1982.

- [34] G. F. Boudreux-Bartels. Time-frequency signal processing algorithms: Analysis and synthesis using Wigner distribution, PhD thesis, Rice University, 1983.
- [35] B. Boashash and P. J. Black. An efficient real-time implementation of the Wigner–Ville distribution, *IEEE Trans.* **35**(11) (1987), 1611–1618.
- [36] V. J. Kumar and C. Carroll. Performance of Wigner distribution function based detection methods, *Optical Eng.* **23** (1984), 732–737.
- [37] S. Kay and G. F. Boudreux-Bartels. On the optimality of the Wigner distribution for detection, in *Proceedings of the IEEE International Conf. on Acoustics, Speech and Signal Processing*, pp. 1263–1265, Tampa, Fl, 1985.
- [38] B. Boashash and F. Rodriguez. Recognition of time-varying signals in the time-frequency domain by means of the Wigner distribution, in *ICASSP*, pp. 22.5.1–22.5.4, 1984.
- [39] B. Boashash and P. J. O’Shea. A methodology for detection and classification of some underwater acoustic signals using time-frequency analysis techniques, *IEEE Trans. Acoustics, Speech Signal Process.* **38**(11) (1990), 1829–1841.
- [40] B. Boashash and P. J. O’Shea. *Time-Frequency Analysis: Methods and Applications*, chapter on Signal detection using time-frequency analysis, Longman Chesire, London, 1992.
- [41] B. Boashash and H. J. Whitehouse. High resolution Wigner–Ville analysis, in *11th GRETSI Symposium on Signal Processing and its Applications*, pp. 205–208, 1987.
- [42] H. J. Whitehouse, B. Boashash, and J. M. Speiser. *High-Resolution Techniques in Underwater Acoustics*, chapter on High-resolution processing techniques for temporal and spatial signals, Springer-Verlag, 1990.
- [43] H. H. Szu. Two-dimensional optical processing of one-dimensional acoustic data, *Optical Eng.* **21**(5) (1982), 804–813.
- [44] P. J. Boles and B. Boashash. *Time-Frequency Analysis: Methods and Applications*, chapter on Applications of the cross Wigner–Ville distribution to seismic surveying, Longman-Cheshire, London, 1992.
- [45] D. L. Jones and T. W. Parks, A high-resolution data-adaptive time-frequency representation, *IEEE Trans. Acoustics, Speech Signal Process.* **38**(12) (1990), 2127–2135.
- [46] N. Marinovic. The Wigner distribution and the ambiguity function: Generalisations, enhancement, compression and some applications, PhD thesis, City University of New York, 1986.
- [47] J. Bertrand and P. Bertrand, Time-frequency representations of broadband signals, in *ICASSP*, pp. 2196–2199, 1988.
- [48] O. Rioul and P. Flandrin. Time-scale energy distributions: A general class extending wavelet transforms, *IEEE Trans. Acoustics, Speech Signal Process.* (1992), pp. 1746–1757.

- [49] R. Altes. Detection, estimation, and classification with spectrograms, *J. Acoust. Soc. Amer.* **67** (1980), 1232–1246.
- [50] T. E. Posch. Wavelet transform and time-frequency distributions, in *Proc. SPIE—Int. Soc. Opt. Engng.* **1152** (1989), 477–482.
- [51] L. Cohen. Generalised phase space distributions, *J. Math. Phys.* **7** (1967), 181–186.
- [52] B. Barkat and B. Boashash. Higher-Order PWVD and Legendre based time-frequency distribution, in *Proceedings of the Sixth IEEE Inter. Workshop on Intell. Sig. Proc. and Com. Systems*, Melbourne, 4–6 Nov. 1998.
- [53] P. Rao and F. J. Taylor. Artifact reduction in the Wigner distribution, in *Proc. of the 32nd Midwest Symp. on Circuits and Systems*, Illinois, August 1989, pp. 849–852.
- [54] A. J. Janssen. Application of the Wigner distribution to harmonic analysis of generalised random processes, PhD thesis, Amsterdam, 1990.
- [55] P. Flandrin. Some features of time-frequency representations of multicomponent signals, in *Proc. of IEEE Inter. Conf. on Acoustic Speech and Signal Processing*, 41.B.1.1–41.B.1.4, San Diego, 1984.
- [56] H. I. Choi and W. J. Williams. Improved time-frequency representation of multicomponent signals using the exponential kernels, *IEEE Trans. Acoustics, Speech Signal Process.* **37**(6) (1989), 862–871.
- [57] Y. Zhao, L. E. Atlas, and R. J. Marks II. The use of cone shaped kernels for generalized time-frequency representation of non-stationary signals, *IEEE Trans. Acoustics, Speech Signal Process.* **38**(7) (1990), 1084–1091.
- [58] M. Amin. *Time-Frequency Signal Analysis: Methods and Applications*, chapter on time-frequency spectrum analysis and estimation for non-stationary random processes, Longman-Cheshire, London, 1992.
- [59] P. J. Kootsookos, B. C. Lovell, and B. Boashash. A unified approach to the STFT, TDS's and instantaneous frequency, *IEEE Trans. Acoustics, Speech Signal Process.* 1991.
- [60] R. G. Baranuik and D. L. Jones. A radically Gaussian, signal dependent time-frequency representation, in *Proc. IEEE ICASSP*, p. 3181–3184, 1991.
- [61] G. Jones and B. Boashash. Instantaneous quantities and uncertainty concepts for signal dependent time frequency distributions, in *Proc. SPIE*, 1991.
- [62] G. Jones and B. Boashash. Generalized instantaneous parameters and window matching in the time-frequency plane, *IEEE Trans. Signal Process.* **45**(5) (1997), 1264–1275.
- [63] B. Barkat and B. Boashash. High-resolution quadratic time-frequency distribution for multicomponent signals analysis, *IEEE Trans. Signal Process.* (1998), (submitted).
- [64] P. Rao and F. J. Taylor. Estimation of IF using the discrete Wigner–Ville distribution, *Electronics Lett.* **26** (1990), 246–248.

- [65] B. Escudie and P. Flandrin. Positivité des représentations conjointes en temps et en fréquence des signaux d'énergie finie; représentation hilbertienne et condition d'observation des signaux, in *rapport GRETSI*, pages 2/1–2/7, 1979.
- [66] D. König and J. F. Böhme. Wigner-Ville spectral analysis of automotive signals captured at knock, *appl. Signal Process.* **3** (1996), 54–64.
- [67] D. C. Reid, A. M. Zoubir, and B. Boashash. Aircraft flight parameter estimation based on passive acoustic techniques using the polynomial Wigner–Ville distribution, *J. Acoust. Soc. Amer.* **102**(1) (1997), 207–23.
- [68] B. Barkat and B. Boashash. Instantaneous frequency estimation of polynomial FM signals using the peak of the PWVD: Statistical performance in the presence of additive gaussian noise, *IEEE Trans. Signal Process.* **47**(9) (1999).
- [69] B. Boashash and A. P. Reilly. *Algorithms for Time-Frequency Signal Analysis*, Chap. 7, Longman Chesire, London, 1992.
- [70] A. Reilly, G. Frazer, and B. Boashash. Analytic signal generation-tips and traps, *IEEE Trans. Signal Process.* **42** (1994), 3241–3245.
- [71] R. Altes. Sonar for generalised target description and its similarity to animal echolocation systems. *J. Acoust. Soc. of Amer.* **59**(1) (1976), 97–105.
- [72] A. W. Rihaczek. *Principles of High Resolution Radar*, Peninsula, 1985.
- [73] A. Dziewonski, S. Bloch, and M. Landisman. A technique for the analysis of the transient signals, *Bull. Seismolog. Soc. Amer.*, (1969), 427–449.
- [74] B. Ferguson. A ground-based narrow-band passive acoustic technique for estimating the altitude and speed of a propellor driven aircraft, *J. Acoust. Soc. Amer.* **92**(3) (1992).
- [75] S. Peleg and B. Porat. The Cramer–Rao lower bound for signals with constant amplitude and polynomial phase, *IEEE Trans. Signal Process.* **39**(3) (1991), 749–752.
- [76] S. Peleg and B. Porat. Estimation and classification of polynomial phase signals, *IEEE Trans. Inform. Theory* **37** (1991), 422–429.
- [77] Z. Faraj and F. Castanie. Polynomial phase signal estimation, *P. EUSIPCO*, 1992.
- [78] B. Boashash and P. J. O’Shea. Time-varying higher-order spectra, *Proc. SPIE*, 1991.
- [79] B. Boashash and B. Ristich. Time-varying higher-order spectra and the reduced Wigner spectrum, *Proc. SPIE*, 1992.
- [80] B. Boashash and B. Ristich. Analysis of FM signals affected by Gaussian AM using the reduced Wigner–Ville trispectrum, in *Proc. ICASSP*, Vol. IV, p. 408–411, Minn. MN, April 1993.

- [81] B. Boashash, P. J. O’Shea, and M. J. Arnold. Algorithms for instantaneous frequency estimation: A comparative study, *Advanced Signal Processing Algorithms, Architectures and Implementations* Vol. 1348, p. 24–46. *Proc. SPIE*, San Diego, Aug. 1990.
- [82] M. Benidir. Characterisation of polynomial functions and application to time-frequency analysis, *IEEE Trans. Signal Process.* **45** (5) (1997), 1351–1354.
- [83] B. Boashash and B. Ristic. Polynomial time-frequency distributions and time-varying higher-order spectra: application to the analysis of multicomponent FM signal and to the treatment of multiplicative noise, *Signal Process.* **67**(1) (1998), 1–23.
- [84] B. Barkat and B. Boashash. Design of higher-order polynomial wigner-ville distributions, *IEEE Trans. on Signal Process.* **47**(9) (1999).
- [85] B. Barkat. Note on the coefficients precision and selection in the implementation of the PWVD, in *Proceedings of the Second Workshop on Signal Processing Applications*, p. 131–134, Brisbane, Australia, 4–5 Dec. 1997.
- [86] P. O. Amblard and J. L. Lacoume. Construction of fourth-order Cohen’s class: A deductive approach, in *Proceedings of Int. Symp. Time-Frequency Time-Scale Analysis*, 1992.
- [87] A. Dandawate and G. B. Giannakis. Consistent kth order time-frequency representations for (almost) cyclostationary processes, in *Proc. Ann. Conference on Information Sciences and Systems*, p. 976–984, 1991.
- [88] J. R. Fonollosa and C. L. Nikias. Wigner higher-order moment spectra: Definition, properties, computation and application to transient signal analysis, *IEEE Trans. Signal Process.* **41**(1) (1993), 245–266.
- [89] A. Swami. Third-order Wigner distributions: Definitions and properties, in *Proc. ICASSP*, p.3081–3084, 1991.
- [90] B. Boashash and B. Ristic. Application of cumulant TVHOS to the analysis of composite FM signals in multiplicative and additive noise, in *Proc. SPIE*, 1993.
- [91] R. F. Dwyer. Fourth-order spectra of Gaussian amplitude modulated sinusoids, *J. Acoust. Soc. Amer.* **90**(2) (1991), 919–926.
- [92] A. P. Petropulu. Detection of multiple chirp signals based on a slice of the instantaneous higher-order moments, in *IEEE 6th Workshop on Statistical Signal and Array Processing*, p. 30–33, 1992.
- [93] L. Stanković. S-class of time-frequency distributions, *IEE Proc. Vis. Image Signal Process.* **144**(2) (1997), 57–64.
- [94] L. Stanković. On the realization of the PWVD for multicomponent signals, *IEEE Signal Process. Lett.* **5**(7) (1998), 157–159.
- [95] B. Senadji and B. Boashash. A mobile communications application of time-varying higher-order spectra of FM signals affected by multiplicative noise, in *Proceedings of the International Conference on Information, Communications and Signal Processing* **3** (1997), 1489–92.

- [96] B. Barkat, L. J. Stankovic and B. Boashash. Adaptive window in the PWVD for the IF estimation of FM signals in additive Gaussian noise, in *ICASSP99*, vol. III, pp. 1317–1320, Phoenix, AZ, March 1999.
- [97] V. Katkovnik and L. J. Stanković. IF estimation using the Wigner distribution with varying and data-driven window length, *IEEE Trans. Signal Process.*, Sept. 1998.
- [98] V. Katkovnik and L. J. Stanković. Periodogram with varying and data-driven window length, *Signal Process.* pages 345–358, June 1998.